

Responses to reviewer's comments

We thank the reviewers for their careful examination of the manuscript. We have responded to each of their comments and suggestions. Our response to each point appears in blue below. The new line numbering refers to the revised PDF produced with latexdiff where the text modifications are clearly marked. **Response to editor at the end.**

In this paper, the authors evaluate a new high resolution ocean/sea-ice model against observations. Such evaluation allows researchers to judge the quality of the model system in particular for future work which is why I in principle recommend publication of this paper.

However, before this paper is accepted, the following issues should be addressed:

1. Throughout this paper, it seems as if observations are seen as the truth which the model must match in order to be credible. However, all these observations have uncertainties, sometimes significant ones, which are not discussed. This needs to be addressed so that readers can understand if a certain mismatch between model and observation is primarily related to issues with the model or might simply be related to observational uncertainty. This includes a discussion of point measurements vs. grid-cell averages for some of the data used.

- The reviewer is correct in noting the absence of discussion around uncertainties in observations for most datasets. A careful examination of the datasets used in the manuscript led the added descriptions of observational uncertainty in the revised text for SSH, T&S, velocity, ice concentration and thickness at lines 299, 349, 378, 429, 448, 472, 481, 510, 521 and 531. Because model evaluation is focused on broad scale statistics, uncertainty of point measurements should not affect the conclusions. However we have included a mention of the undersampling problem at lines 380, 449 and 511. Due to issues with melt pond detection in the sea ice concentration product used in this manuscript, we switch from total ice area comparisons to comparisons of total ice extent (section 3.3.1), which is a more robust metric.

2. Throughout this paper, for any model-data mismatch there is too little discussion of possible error sources that are not related to the representation of physics in the model itself. Such error sources include internal variability, issues with the forcing, issues with the lateral boundary conditions, issues with spin up, etc. Without such discussion, it is again hard to judge how severe (or not) model-data mismatches are.

- Impacts of error in model physics and numerics, or impacts due to improvement in these aspects, are clearly indicated by differences in various hindcast results. Lateral boundary condition and mixing parameterization follow common practice in ocean modelling, so we simply document the approaches being used. Model initial conditions are taken from either high-resolution reanalysis product or a global solution with known bias, so no special spin-up is performed. A discussion on impact of using different atmospheric forcing is added at line 623 when comparing differences between CREG12 and T321 results. We have added a description of the river forcing at line 253.

3. Throughout this paper, there is no discussion of the tuning of the model. Hence, it is not possible to judge if a certain mismatch (or a certain agreement) between model and data was achieved because a particular data set was used to tune the model or whether the agreement is indeed an achievement of the model. This holds in particular for the discussion of sea ice, where slightly different tuning of, say, surface albedo might change the ranking of the different model versions significantly.

- The tuning of the model was kept to a minimum. In most respect, the same parameters used in ORCA12-T321 were used in the CREG12 experiments. In CICE, except for explicit parameters discussed in Section 2.1.5 related to the dynamics, the default parameters and physics were used. Text added at lines 190-200.

4. Validation of an ocean/sea-ice model system is not possible, evaluation however is. The terminology should be changed throughout this manuscript. Compare Oreskes, Naomi, Kristin Shrader-Frechette, and Kenneth Belitz. "Verification, validation, and confirmation of numerical models in the earth sciences." *Science* 263.5147 (1994): 641-646.

- Thanks for this precision. "Validation package" has been replaced by "verification package" and "validation" in general by "evaluation".

Minor comments:

p.2, l.3: It sounds odd that the government of Canada is developing a model. Usually, one would assume that the government has other issues to deal with than climate-model development :-)

- corrected at line 2.

p.2, l.6: Is there a reason for using the judgemental term "ice infested"?

- The same expression was used in Lemieux et al. (2015), QJRMS. It is appropriate in terms of navigational safety, which is one of the priorities of the prediction system.

p.6, l.7: Do you mean "tuning" in the sense of parameter adjustments or in the sense of model development? The latter seems to be the case, but common usage of the term "tuning" implies the former.

- Text is revised to use "improvement" instead of "tuning".

p.6, l.20: If the surface layer is just 1 m thick, what happens when the ice thickness becomes larger than 1 m?

- The "levitating ice" hypothesis applies throughout the paper (see also conclusions where reference is made to the opposite "embedded ice" hypothesis). In the "levitating ice" paradigm,

the ice does not penetrate into the ocean but "floats" above, which has implications in terms of volume and water and salt exchanges. Text added at lines 152-157.

p.6, l.11: This seems to be a repetition of the information p.5, l.23

- True, statement removed.

p.9, l.8: Can you provide a few more details on this approach?

- This is related to point p6l20 where we have explicited the "levitating ice" paradigm. See modified text at lines 152-157.

p.9, l.23: What is the volume of observations?

- The question refers to the volume observations used in the CGRF forcing. The answer is unfortunately outside the expertise of the present authors and the scope of this contribution. We refer to Smith et al. (2014) and the references therein. For instance, further details can be found in Belair et al. (2006). We can grossly say that the World Meteorological Organization organizes a common operational data feed to all participating centres. The core of it includes thousands of full-depth radiosonding carried out twice a day, thousands of ground stations, some data from aircrafts and an increasing number of satellite derived information, mainly radiance at the top of the atmosphere which however runs typically nowadays in the million points a day but where is their infancy in 2006 and almost non-existent at the beginning date of the CGRFs (2002). The total volume would have run in the 10^5 at the beginning of the CGRFs and close to 10^6 by the end, excluding thinning of the data during their ingestion.

p.13, l.17ff: Why is not the same data set used for both mean and fluctuations?

- Satellite altimeter provides sea level anomalies (SLA). This yields the information for fluctuations in sea level. However, the information on the geoid is required in order to estimate the mean (the true neutral surface for the dynamics, the geoid, is not spherical; hence the SSH measured from the altimeter can not be used alone for the investigation of the mean). Hence the mean field is provided as a separate dataset, here the CNES-CLS09 (Rio et al., 2011) MDT (blended with the mean of the altimetry SLA over the study period). These geoid models are constantly refined as well which makes difficult their inclusion in the processing of the altimeter data. For the 3D ocean models such as the one presented in this manuscript, the geoid is considered flat, that is, the model is at rest when SSH is a constant everywhere. The information provided in Section 3.2.1 p.13 seems sufficient although a clear understanding of the present issue is a complex undertaking.

Section 3.2.3: T and S are of importance not least because they determine the density profile. Would be good to compare density in model and observations.

- Yes and no, density would be certainly of interest to determine the circulation (if considered a Lagrangian surface), but in general the analysis of model-obs of density will be redundant with T&S.

p.19, l.26: I expect that it is much harder to get the trend roughly right than the actual area (which can easily be adjusted by tuning). I hence disagree with the statement that H05 is better than H02 or ORCA12-T321 on this metric.

- While we agree on the general statement on the adjustment by tuning of the total ice area and on the difficulty of getting the trend correct, we disagree on the statement that our metric is not sufficient for a conclusion. Our conclusion is based on the improved seasonality and September ice extent (please note that we have switched from “ice area” to “ice extent” in the manuscript for better robustness). This sentence does not address the overall trend which is agreedly better in H02 (see next sentence p.20.l.1 for this). However, at least in terms of ice extent alone, Fig12b does show that in terms of September value, H05 performs better over the 2005-2009 period (hence excluding the spinup period and the pathological behaviour after 2009 also mentioned in the manuscript). Finally, showing the total ice extent after 2009 for H05 (we extended a bit the run compared to the other hindcasts) may bias the reader against H05, in terms of overall trend. The resulting “appropriate” 2005-2009 period for comparison is then too short to be statistically significant to our minds.

p.20, l.1: The trend is negative but not necessarily decreasing section 3.3.2: Would be interesting to compare the seasonal cycle of obs. vs. model

- Thanks, will correct trend to "negative". One problem that constrains a seasonal cycle exercise is that ice in H02 is mostly in equilibrium at the start of the simulation (again a question of similarity of model configurations with the used IC) whereas that of H05 is clearly not, going through a quick adjustment period (2 years). The overall hindcast period is also short, so removing the first 2 years reduces the construction of the climatology to 2005-2009 (5 years), which we feel uncomfortable to describe as climatological seasonal cycle.

Fig. 1: Is the coast line in the figure the model coast line or a plotting-program coast line? The former would be better.

- The latter. The plotting-program-provided coastline is actually a little coarser than the actual model coastline because of the high resolution (2-5 km) of the model in the Arctic. However, this difference of detail would be too fine in maps to be distinguishable.

Fig2ff: Would be helpful if always the model is shown first and then observations (or other way around), rather than sometimes showing model first and sometimes showing obs first.

- Corrected (see Figures 3, 4, 10 and 11).

Fig2ff: Labels of many figures are too small

- Corrected in Figures 3, 4, 6, 7, 10, 11 and 14.

Fig.7: It might be helpful to harmonise the total range of the individual subpanels to allow for a visual judgement of absolute mismatches.

- We have tried but found that this was not reflecting, for instance in the Arctic, subtle, but important in terms of hydrography, vertical variations in temperature.

Typos etc.

p.3, l.20: communities' >>> corrected

p.4, l.6 : no comma after period >>> corrected

p.6, l.20: 450 m >>> done

p.6, l.28: dependence >>> done

p.7, l.16: This is commonly referred to as a 3-layer model (2 ice + 1 snow) >>> yes, corrected

Anonymous Referee #2

Received and published: 17 February 2015

Overview

In this article the authors introduce a new North Atlantic-Arctic ocean-sea ice modelling system and detail several different incremental test configurations. For each configuration a hindcast experiment is performed and these are assessed using some useful tools in order to ensure the model is fit for operational running. I think that the documentation of this system and evaluation of the model is of interest to the scientific community and therefore recommend that this paper is published in GMD subject to the points below being addressed.

General comments

* In general I think that a bit more care is needed when describing the comparisons with observations. In particular it is often unclear exactly what is being compared with what (i.e. are we comparing the mean of the observed values with mean of model values, or are the model values interpolated to observation locations or what?). This is particularly true for Figures 7, 9, 10, 11 and 14.

- We have added text to make the comparisons clearer for each of these figures.

* More explanation is needed in introducing the model experiments. In particular it is not clear how the multi-category ice fields are initialised in your H05 CICE run?

- We believe that the statement on page 11 lines 5-7 is sufficient.

* The development of this model is clearly motivated by the need 'to provide Canada with short-term ice-ocean predictions and hazard warnings' which will presumably be done using an operational analysis-forecast system. However nothing is said about how this will be run. In particular data assimilation is mentioned and so is coupling to the Environment Canada's regional weather prediction system but will both these things be done together (i.e. are you planning to implement a fully coupled data assimilation system)? I think that if there were a little more information in the Introduction and Conclusions sections about these plans then it would help the paper to highlight the paper's relevance.

- Unfortunately, this contribution is not aimed at presenting details (including analysis) of the ice-ocean prediction system (which is not ready yet), not to mention details of the long-term planned coupled atmosphere-ice-ocean prediction system. However, we have amended the text at line 47 to reflect this. The coupled atmosphere-ocean data assimilation is certainly a hot topic that we cannot really address at this stage.

* There are a number of instances of 'PSU' in the text and on the figures in relation to salinity which should be removed. There is no such thing as a Practical Salinity Unit (PSU) because, when measured on the practical salinity scale, salinity is simply a dimensionless ratio. Therefore you should give your salinity as numbers with no units. Strictly speaking you should simply state somewhere that "salinity is measured on the practical salinity scale" but one could argue that this is not really necessary these days because everybody measures it this way(?).

UNESCO (1985) The international system of units (SI) in oceanography, UNESCO Technical Papers No. 45, IAPSO Pub. Sci. No. 32, Paris, France

- We followed the reviewer's suggestion throughout the text and figures.

* Finally I presume the journal language is English (not US English) in which case there are a few misspellings such as 'programs' and 'modeling' instead of 'programmes' and 'modelling'.

- Absolutely right! We use though Canadian English which may depart from UK English in a couple of occasions.

Specific comments

p5.l24-5: NEMO is not really "an ocean and ice model" it is much larger than that (inc. passive tracers, biology, etc.). NEMO contains an ice model called LIM but this isn't technically NEMO. Given this is under consideration for the NEMO Special Issue it might be worth ensuring this is correct? The NEMO book says: "The Nucleus for European Modelling of the Ocean (NEMO) is a framework of ocean related engines, namely OPA for the ocean dynamics and thermodynamics, LIM for the sea-ice dynamics and thermodynamics, TOP for the biogeochemistry (both transport (TRP) and sources minus sinks (LOBSTER, PISCES)). It is intended to be a flexible tool for studying the ocean and its interactions with the other components of the earth climate system (atmosphere, sea-ice,

biogeochemical tracers, ...) over a wide range of space and time scales.”

- The reviewer is correct. See modifications at Section 2.1.2. We now describe NEMO as a bio-physical multi-component system, with OPA as the ocean model component.

p7.14: I think it would be clearer to include units for the viscosity ($1\text{e-}4\text{ m}^2/\text{s}$) even if they are the same as for the following diffusivity ($1\text{e-}5\text{ m}^2/\text{s}$)

- done

p7.18-9: you say “hindcast H05 requires a decrease to 180 s after July 2007 to ensure stability in Dease Strait.” Why is this? Was this expected or just a blow-up? The use of “requires” rather than “required” here implies that this was foreseen rather than reactive.

- The reviewer's hunch is correct. Corrected.

p8.11-4: the coupling of NEMO and CICE within the Met Office’s coupled model HadGEM3 is described by Hewitt et al. (2011) and within the ocean-ice FOAM system by Blockley et al. (2014) (although the latter mainly links back to the former). Can these not be cited instead (or as well) as the pers. comm. (see references below)? Section 3.1: How are the multi-category CICE initial conditions produced for H03-5?

- The reviewer is correct. Text modified accordingly at line 146. CICE initial conditions are described in page 11 line 5-7 as already mentioned.

Section 3.2: Why is there no specific validation of SST? There is a large number of SST data (both in-situ and satellite) that would be useful to compare against the model. At the very least it would be informative to compare against L4 gridded data products such as OSTIA (also available through MyOcean).

- Yes, we did the SST comparisons with the OSTIA product but did not include them in this manuscript. There were some redundancy with the upper ocean comparison and the decision was made to not include them.

p15.110: Regarding surface circulation comparisons with drifters you say: “The general agreement is remarkable”. I think that “remarkable” is perhaps a little strong here. The agreement is pretty good but it’s difficult to make a “remarkable” visual comparison between a $1/12$ degree and a $1/2$ degree field. Perhaps the model output could be regridded to $1/2$ degree for a more direct comparison?

- We have corrected the expression and followed the reviewer suggestion of upscaling the model results to $1/2$ degree for a more direct comparison. See modified paragraph at lines 345.

p16.l2: how does the number of data in your modified CORA3.4 data set compare with the ERA-CLIM funded 'EN4' data set of Good et al. (2013) (see references below)?

- Both products contain similar datasets. The QC procedures probably differ a bit between them, but there shouldn't be a big difference using either for the evaluation.

p17.l18: be careful with the use of “significantly” here. Do you mean statistically significant? If not then “considerably” might be better. However I am confused as to why this should even be described as considerable given that just before (p17.l10) you describe the temperature biases as “very small (less than 0.5 deg. C)”?

- There was no statistical tests and we have therefore followed the suggestion of the reviewer. The text was improved. "very small" -> "small". "significantly" replaced by “considerably” as per reviewer's suggestion.

p17.l27: “In order to investigate whether these recent variations are reproduced...”. It is not clear to me what the “recent variations” are. Could this sentence be reworded?

- This statement relates to "the recent increase" of line 26. “these recent variations are” replaced by “this increase is” at line 424.

p18.l21: You say: “the temperature and salinity gradients across the strait are broadly similar.” I don't think this is true. Certainly it looks like the temperature difference across the strait is the same but the gradient is not as the values are quite different in the middle of the strait where the model is cold-biased. This cold bias is mentioned later (p18.l25-6) but I think it should be mentioned sooner around l21.

- The reviewer is correct. The original intention was to signify that the temperature difference between the east and west sides of the strait is similar, and we have amended the wording accordingly. We have also made earlier mention of the cold bias in the middle of the strait.

p20.l1: “decreasing trend” is not necessarily true. Certainly the trend is downward but “decreasing trend” suggests that the gradient of the trend is negative! Additionally I am not sure that the gradients of these lines are that similar either. There is a general reduction in ice area in H02 and T321 but they don't really capture the 2007 minima very well? Furthermore (and see comments for Figure 12) it looks like the CICE run H05 may be adversely affected by its initial conditions because it drops off pretty rapidly save for the increase in 2008/9. Do you think this model is still spinning up?

- The reviewer is correct for the trend. See response to Rev#1. The ice in H05 is likely spun up (in terms of thermodynamics) after 2 years as stated in the text. Then, the model dynamics accumulate too much thick ice in the Beaufort Gyre which starts to show in the total ice area after 2009.

p20.l25-28: “The model ... tends to overestimate the thicker ice categories in the Beaufort Gyre and underestimate them near the North Pole.” The converse is also true (i.e. that the model underestimates thicker categories in Beaufort Gyre and overestimates them near pole). Should this be mentioned? How does this compare with the single-category LIM ice fields in H02? I suspect that it is much better but it should be mentioned (but not necessarily plotted). Are the results in Figure 15 consistent with Figure 14?

- For comparison with LIM2, we prefer to look at the ice thickness retrieved from ICESat. We fear a typo in the reviewer's "converse" argument. We believe she/he meant the "thinner" categories. Yes, this is now mentioned at line 526. Grossly speaking: yes, Figures 14 and 15 are consistent.

p21.l17-18: It might be worth mentioning that this over-estimation of volume with NEMO-LIM2 is fairly well known being consistent with the findings of Blockley et al. (2014) and Massonnet et al. (2011)

- Thanks for the references. Wang et al. (2008) [added reference] found that ice area and volume on LIM2 is linear with the parameter hiccrit. The "over-estimation" is therefore not systematic but tends to be an artifact of people using generally a (too) large value for hiccrit. Text modified accordingly at lines 168-174.

Section 3.2.2 (Figure 19): I am not a fan of the use of “average bias” when talking about directional vector quantities such as ice velocity. The main reason for this is that it is difficult to interpret what a positive or negative bias actually means unless the underlying field is entirely uni-directional. For example a positive bias (say) could mean that your velocities are too strong in a eastward regime or too weak in an westward regime. Furthermore if the observations cover an area with ice moving in both directions then it’s even more difficult to understand what a positive bias means and what the effect of (possible) compensating errors might be. Therefore I think this piece of text (the interpretation of Figure 19) needs some more careful explanation. Perhaps it might be better to try to understand the errors by using an RMS error time series in Figure 19 and then show the biases spatially? The ice drift maps in Figure 18 would be useful here if we knew where the in-situ observations actually were?

- The reviewer is globally correct. However, we have some confidence that after studying the mean March ice circulation (Fig.18) that we are mainly looking at differences in the intensity of this circulation, and that therefore it is legitimate and meaningful to investigate the bias in velocity magnitude. To complement this, we have also looked at the RMS of the velocity vector differences (i.e. summation of $\| \mathbf{v}_{\text{mod}} - \mathbf{v}_{\text{obs}} \|^2$) which yields similar results and ranking. We however amended the text at line 561 to reflect this.

p21.l15: Re. comparisons with PIOMAS in Figure 17 you say “The seasonal cycle (Fig.17, top panel) for H05 is very close to the PIOMAS value”. Although the magnitudes do look very similar there does appear to be a “lag” in your time series whereby the onset of ice growth AND melt is slightly offset temporally. This is not mentioned in the text at all. Do you have any idea why this might be the case?

- The reviewer is correct. There is about a one month lag, now stated at line 537. PIOMAS uses the NCEP forcing which seems to be uncorrected (see Large and Yeager's analysis, 2004 and Hunke's, 2007). We can only speculate if this is sufficient to explain the lag.

p22.l23: You say “due to Ekman transport acting of the ocean” which doesn’t quite make sense. Do you mean “Ekman transport acting on the ocean” or something like “Ekman transport within the ocean”?

- "of" replaced by "on". The expression is ill-posed but tries to discriminate the portion of Ekman transport which is at play in the ice and in the ocean. One could see the Ekman spiral process as being applied to the combined ice-water system.

p25.l16-17: You say you are hoping to increase the ocean vertical resolution to 75 levels to put you “on par with DRAKKAR and Mercator-Océan’s latest standards”. Is this true? I thought Mercator’s vertical resolution was 50 levels not 75? It is certainly listed as 50 in Drillet et al. (2014) and Tonani et al. (2015).

- Not all MERCATOR operational systems incorporate indeed 75 vertical levels but this is the goal. The latest GLORYS analyses (2v1 and 2v3) were produced with 75 levels for instance and 75 levels is the standard in research mode (DRAKKAR). Thus, to satisfy the reviewer, we suggest to add the expression "in research" at line 650.

Figure 4: please change “modeled” to “modelled”.

- done

Figure 5: It is nice to see the high resolution data in the bottom plot. However the fact that one is 1/2 degree and the other 1/12 degree does make it hard to draw comparisons. Have you coarsened the 1/2 degree model output to 1/2 degree to compare directly? It might be nice to include another image here showing the regridded currents?

- Done.

Figure 6: please remove “PSU” from salinity colourbars

- Done

Figure 7: It is unclear exactly what is being plotted here. For each of these boxes are you comparing the average of all observations with that of all the model points? Or are the model profiles collocated with the observations (either interpolated to obs locations or nearest grid cell)? Please remove “PSU” from salinity axes.

- Text added at line 397-402 and in the figure caption. The reviewer's second guess is correct. The model is collocated in time and space with the observations and then both are averaged horizontally and in time to yield a single profile per box. "PSU" removed as per reviewer's suggestion.

Figure 8: What does the white missing data mean here?

- It is regions where salinity exceeds 34.8 over the whole water column. Included in the caption now.

Figure 9: The grey shaded area is really not very visible when this paper is printed out (although ok looking on screen). I would recommend adding dashed/dotted lines at the max/min extents of the grey to emphasise it. Also the differences between the black Proshutinsky et al. (2009) data set and your coloured lines are not explained. Yours looks very different from their with much more fluctuation. Is it simply a case of using a different temporal discretisation (i.e. monthly vs. yearly)? Either way this should be addressed. Figure 10/11: Same question as Figure 7. How are the model-obs values calculated? Are you comparing means of point observations model means and if so how are they collocated? Please remove "PSU" from salinity axes.

- Dashed lines added to Fig.9 as per reviewer's suggestion. Indeed, the modelled lines are monthly values whereas the observations are only valid for the summer period. Text added a line 430. Therefore the model values include a seasonal cycle which is not present on the observations. No collocations was involved in this plot as Proshutinsky et al. (2009) provides an estimate for the entire region with error bars. The region of integration is also clearly defined in the same paper. See added text.

Figure 12: Your CICE/H05 experiment starts with a relatively poor representation of September Arctic ice area and drops off rapidly. Is this an artifact of the initial conditions? Do you think this model is still spinning up? It would be interesting to know how the 10 ice categories were initialised in your H05 run.

- Yes, ice in H05 adjusts in a 2-year period to the initial condition. See above response.

Figure 14: It would be useful to explicitly state what "difference" means here (i.e. modelled-observed?)

- added.

Figure 15/16: As mentioned above this over-estimation of ice volume in LIM2 is well known (Massonnet et al. / Blockley et al.) As mentioned above your H05 volume time series appears to have a time lag in it but this is not discussed.

- see above response for p21.117-18 and p21.115.

Figure 18: What is the resolution of the NSIDC observational product? This is not mentioned in the text either. How realistic is the circulation in the Beaufort Gyre in this NSIDC product? It doesn't look very pronounced (but this could be answered by the resolution of the product above).

- NSIDC product has a resolution of 25km. It is sufficient to resolve the circulation in the Beaufort Gyre. It is however a bit negatively biased as shown in Fig.19, possibly related to the methodology employed. The CERSAT estimate is somewhat faster (but still slower than any modelled ice drift) and a little noisier but does not cover as many regions (not shown).

Figure 19: As discussed for Section 3.2.2 above I think some more work is needed to understand the information in this figure.

- Texts added at lines 561 and 566. See also response to Rev#2 Section 3.2.2.

Minor typos etc.

p2.l9: "model represent" should be "model represents" or "model represents" >>> Corrected
p3.l22: "program" should be "programme" (unless it's a computer program) >>> done
p5.l15: "re-increasing" is not very good English and should be replaced >>> corrected
p6.l1: please remove "very" as "substantially" shouldn't need any further quantification >>> done
p15.l23: "myOcean (www.myOcean.eu)" should be "MyOcean (www.myocean.eu)" >>> done
p15.l26: "program" should be "programme" >>> done
p16.l2: "programs" should be "programmes" >>> done
p16.l3: "programs" should be "programmes" >>> done
p16.l17: please remove "PSU" >>> done
p16.l20: please remove "PSU" >>> done
p17.l5: please remove "PSU" >>> done
p17.l6: please remove "PSU" >>> done
p18.l28: "maximums" should be "maxima" >>> corrected
p19.l21: "coefficents" should be "coefficients" >>> done
p20.l5: "adjusement" should be "adjustment" >>> done
p22.l15: I don't like winds being described as "large". This should "high winds" or "strong winds" (or perhaps "large wind stresses"?). >> done

Response to further comments/suggestions from the editor:

Thanks a lot for the in-depth reading and proof-checking of the manuscript. Please find below our responses to your comments. We apologize for not being able to reproduce in full the editor's comments.

1-Manuscript types: The manuscript was submitted as "Technical, Development and Evaluation

papers", which still seems to be appropriate, unless mistaken. The first one, "Model Description paper" that you were alluding to, seems too specialized to a new version of one particular model, which is obviously not our case, NEMO3.1 and CICE4.0 being already superseded by newer versions (mentioned in the conclusions of our paper). Additionally, the evaluation aspect of NEMO in the North-Atlantic and Arctic oceans is the most prominent aspect of our contributions. We have moreover no problem with providing the code and the namelists of our experiment in electronic supplements. Please advice if we are mistaken.

2-p13l416, "considerably" changed for "noticeably" as suggested

3-p13l431, more details is now provided. The uncertainty was actually directly provided by Proshutinsky in 10^6 km² (pers comm. 2013). We merely translate it to percents.

4-p14l497, sentence added as per editor's suggestion

5-p14l498-500, reference to the initial condition section for sea ice added

5-p16l523-527, averaging period added

6-p16l540, more details added to the description of the error in the total ice volume computed from PIOMAS.

7-p17sec3.3.2.

0) the paragraph has been rewritten, adding for instance a discussion of the source of errors, which was missing from the revision 1.

a) assertion that H05 was better than H02 was indeed not backed up by Fig.18! An error was introduced when testing a new plotting program and the wrong plot was inserted for H02 in Fig.18. The new figure now reproduces the assertion that H02 has all reasons to exhibit a more intense ice circulation relative to ORCA12-T321 and H05 (i.e., over-estimated ice-air wind stress compared to ORCA12-T321 and larger air-ice drag coefficient relative to H05). We apology for the error.

b) "velocity" used instead of drift for harmonizing the manuscript, except in one occasion where "drift" was used to described the buoys (i.e. "drift" is what is observed from a Lagrangian perspective).

c) l557, "at 25 km resolution" moved up as per editor's suggestion

d) l563, we are sorry to disagree here. "Products" seems to be the most appropriate expression to describe the ensemble of both data-derived products and several model hindcast outputs (a model product). Note that we do not support the use of the expression "data" when referring to model output. It is an abuse of terminology that observationists hate to read in modelling papers...!

8-references (smith et al., 2014; Belair et al., 2006) added to the text as per editor's suggestion

9-abstract: semicolons replacing periods.

10-p2l28, parenthesis moved up

11-p6l163, "as in" replacing "including"

12-p10l305, "SSH AVISO anomalies" replacing "SSH anomalies"

13-p11l346, "corresponding to" replacing "corresponding with"

14-p14l447, "of "one-month lag" replacing "a month lag"each instrument" replacing "for each instrument"

15-p15l489, "to ease comparison, ORCA12T321 output is considered only on the CREG12 domain" replacing "to ease data exchange and comparison, ORCA12T321 was provided too on the CREG12 grid". Note that we have replaced "data" by "output" in the editor's suggestion (see also point 7d above).

16-p16l532, period mentioned in caption of Figure 16 added to the text.

17-Fig16, correction on "ICESat".

18-p17l544

A high-resolution ocean and sea-ice modelling system for the Arctic and North Atlantic Oceans

Frédéric Dupont¹, Simon Higginson², Romain Bourdallé-Badie³, Youyu Lu⁴, François Roy⁵, Gregory C. Smith⁶, Jean-François Lemieux⁷, Gilles Garric⁸, and Fraser Davidson⁹

¹MSC, Environment Canada, Dorval, QC, Canada

^{5,6,7}MRD, Environment Canada, Dorval, QC, Canada

^{2,4}Bedford Institute of Oceanography, Fisheries & Oceans Canada, Dartmouth, NS, Canada

^{3,8}Mercator-Océan, Toulouse, France

⁹Northwest Atlantic Fisheries Centre, Fisheries & Oceans Canada, St. John's, NF, Canada

Correspondence to: F. Dupont
(frederic.dupont@ec.gc.ca)

Abstract. As part of the CONCEPTS (Canadian Operational Network of Coupled Environmental Prediction Systems) initiative, a high resolution (1/12°) ice-ocean regional model is developed covering the North Atlantic and the Arctic oceans. The long-term objective is to provide Canada with short-term ice-ocean predictions and hazard warnings in ice infested regions. To evaluate the modelling component (as opposed to the analysis –or data-assimilation– component, which is not covered in this contribution), a series of hindcasts for the period 2003–2009 is carried out, forced at the surface by the Canadian Global Re-Forecasts. These hindcasts test how the model represents upper ocean characteristics and ice cover. Each hindcast implements a new aspect of the modelling or the ice-ocean coupling. Notably, the coupling to the multi-category ice model CICE is tested. The hindcast solutions are then assessed using a verification package under development, including in-situ and satellite ice and ocean observations. The conclusions are: 1) the model reproduces reasonably well the time mean, variance and skewness of sea surface height; 2) The model biases in temperature and salinity show that while the mean properties follow expectations, the Pacific Water signature in the Beaufort Sea is weaker than observed; 3) However, the modelled freshwater content of the Arctic agrees well with observational estimates; 4) The distribution and volume of the sea ice is shown to be improved in the latest hindcast due to modifications to the drag coefficients and to some degree to the ice thickness distribution available in CICE. 5) On the other hand, the model still overestimates the ice drift and ice thickness in the Beaufort Gyre.

1 Introduction

The CONCEPTS (Canadian Operational Network of Coupled Environmental Prediction Systems) initiative has fostered collaborations between different federal departments (Fisheries and Oceans Canada, Environment Canada and the Department of National Defence) that yielded the development of several operational prediction systems. These include a coupled (atmosphere-ice-ocean) Gulf of Saint-Lawrence system (officially operational since June 2011, Smith et al., 2012), the Global Ice-Ocean Prediction System (GIOPS, run in real-time since March 2014, Smith et al., 2015), a Great Lakes coupled system (still in development, Dupont et al., 2012), a regional ice-only prediction system (~~run in real-time since July 2013~~, (run in real-time since July 2013, Lemieux et al., 2015a) and a regional Arctic-North Atlantic ice-ocean system based on the CREG12 (Canadian REGIONal) configuration with a nominal horizontal resolution of $1/12^\circ$. The latter is the focus of this paper. The GIOPS, Great Lakes and CREG12-based systems are based on NEMO (Nucleus for European Modelling of the Ocean, <http://www.nemo-ocean.eu>), while the coupled Gulf of Saint-Lawrence system has just been transitioned to NEMO for the ice-ocean component. The development of these systems has benefited greatly from a collaboration with Mercator-Océan in France.

The goal of the regional system based on CREG12 is to provide Canada with short-term ice-ocean predictions and analyses covering parts of the North Atlantic and whole Arctic oceans at high resolution. For this purpose, the regional system will eventually be coupled to the regional weather prediction system and wave prediction system of Environment Canada. The coupled system is expected to improve regional weather and marine forecasting services such as issuing bulletins and warnings in ice infested waters for navigation, energy-exploration and northern communities' requirements. As such, the system development has benefited from financial support from the Canadian METAREA programme and the Beaufort Regional Environmental Assessment (BREA) project. However, before the full system (analysis+forecast) can be approved for operational use, we need to understand how to use the forecasting component to its full potential, following the best practices of the community running at comparable resolutions. Hence, a series of hindcasts was performed using the forecasting component, each implementing and testing a different aspect of ocean-ice modelling. Implementation of data-assimilation in this prediction system, adopting the same methodology as in Smith et al. (2015), is under development and will be reported in follow-on contributions.

These hindcasts are not long enough to test the full robustness of the model in preserving observed water and ice properties at climatic scales (i.e. several decades), as the initial conditions still imprint the model state after 8 years. Nevertheless, discrepancies between atmospheric forcing products and differences in upper-ocean and ice physics are sufficient to create diverging upper-ocean and ice states and variabilities in this short period that are worth investigating. Moreover, recent satellite missions and extensive and automatized observing in-situ programmes (ARGO floats and ice-tethered profilers to cite a few) create a wealth of data covering the hindcast period which we take advantage of in our evaluation approach. We are therefore testing the mean state of the model using a few vari-

ables, sometimes focusing on some integrated indices over time, or more extensively mapping the model-observation discrepancy in space and time.

In this contribution, we describe the model components and the verification strategy, along with results of the evaluation of the latest hindcast. The objective is to present to the community the progress made and challenges met in developing a high resolution modelling system for the Arctic-Atlantic oceans, in the spirit of Megann et al. (2014). In assessing the performance of the latest hindcast in terms of ice properties (concentration, thickness and velocity), we include comparison with an intermediate hindcast and the $1/12^\circ$ resolution equivalent global simulation ORCA12-T321 of Mercator-Océan.

More precisely, Section 2 is divided into the description of the model (domain, model components and parameters; Section 2.1), the input bathymetry and other initial and boundary conditions (Section 2.2), and the description of the verification package (Section 2.3). Section 3 provides details of the hindcast simulations (Section 3.1), then describes the simulation results in terms of the statistics of the sea surface height, the hydrography and the general circulation (Section 3.2) and in terms of sea-ice metrics (concentration, thickness, volume and drift; Section 3.3). Section 4 concludes.

2 Model setup, input data and verification package

2.1 Model description

2.1.1 Domain configuration

The global ORCA12 domain (ORCA family grid at a nominal horizontal resolution of $1/12^\circ$ in both longitudinal and latitudinal directions, Drakkar Group, 2007) is used to derive a seamless (i.e., the "north-fold" discontinuity of the global grid is removed) regional domain covering the whole Arctic Ocean and parts of the North Atlantic down to 27°N . The horizontal grid consists of 1580×1817 points on which resolution varies from 8 km at the open boundary in the Atlantic Ocean to an average of 5 km in the Arctic, and down to slightly below 2 km in some of the southern channels of the Canadian Arctic Archipelago (Figure 1).

The spatial variation of the first Rossby radius of deformation is shown in Figure 2a. From about 40 km along the southern Atlantic boundary down to a few kilometers in the Labrador Sea, the Greenland, Iceland and Norwegian (GIN) seas and continental shelves, the radius increases again in the deep Arctic Ocean to above 10 km. Relative to the local resolution (Figure 2b), the model resolves –grossly speaking– baroclinic eddies in the Sargasso Sea and the Azores region where there are at least two grid spacings for resolving the Rossby radius, but becomes eddy-permitting in the Labrador Sea (one grid spacing) and less than permitting in the GIN seas (under one grid spacing). However, the model is again eddy-resolving in the central Arctic Ocean, which is of importance for the present application.

90 2.1.2 Ocean component

The ocean component is taken from version 3.1 of NEMO with some code additions from Mercator-Océan, the UK Met Office and the DRAKKAR community. NEMO is a biophysical ocean-ice multi-component system developed originally in Europe (Madec and NEMO team, 2008), that has evolved substantially since its introduction in the 2000s. The ocean engine of NEMO is the primitive equation model OPA (Océan Parallélisé; Madec et al., 1998) adapted to regional and global ocean circulation problems. It is intended to be a flexible tool for studying the ocean and its interactions with the other components of Earth’s climate system over a wide range of space and time scales (Masson-Delmotte et al., 2006; Drillet et al., 2005; Barnier et al., 2006). An advantage of the NEMO model is its widespread use and continuous improvement by the scientific community (Rattan et al., 100 2010).

Previous versions of NEMO have been extensively tested and applied in Canada for global, basin and regional applications (Holloway and Wang, 2009; Zhu et al., 2009; Wang et al., 2010; Lu et al., 2014).

2.1.3 Ocean model parameters

105 We started from the configuration and parameters of the $1/12^\circ$ resolution equivalent global simulation, ORCA12-T321 of Mercator-Océan, which are described below and notes will be made when departing. NEMO is run with the implicit free-surface solver and linear free-surface (a version using a time-splitting approach and a non-linear free-surface, including the simulation of the main constituents of the tides, is presently being evaluated). The present version uses the same 50 vertical 110 z-levels used in GIOPS, with spacing increasing from 1 m at the surface to 450 m at 5000 m. Bottom partial steps are employed for an accurate representation of the varying bathymetry. The tracer advection uses the Total Variance Diminishing (TVD) scheme. The vectorial form for momentum is chosen, allowing conservation of both energy and enstrophy. The lateral diffusion operator is biharmonic for momentum along geopotential surfaces and harmonic for tracers along isopycnal surfaces. 115 The biharmonic viscosity has a nominal value of $-1 \times 10^{10} \text{ m}^4 \text{ s}^{-1}$ at the southernmost point, and is scaled by the third power of the grid spacing over the rest of the computational domain. The harmonic diffusion coefficient for tracers follows the same resolution-dependence principle, with a nominal value of $50 \text{ m}^2 \text{ s}^{-1}$ and a linear scaling. For momentum, we additionally tested the purely free-slip and no-slip lateral boundary dynamic conditions, but retained the former one for most of the hindcasts. 120 The background values for vertical viscosity and diffusivity are $10^{-4} \text{ m}^2 \text{ s}^{-1}$ and $10^{-5} \text{ m}^2 \text{ s}^{-1}$ respectively. We have also experimented with the turbulent kinetic energy (TKE; Gaspar et al., 1990; Blanke and Delecluse, 1993) and generic length scale (GLS; Umlauf and Burchard, 2003) closure schemes. The bottom drag is quadratic with a fixed non-dimensional coefficient of 10^{-3} . The model time step is 360 s for all hindcasts (including ORCA12-T321), except for hindcast H05 that required

125 a decrease to 180 s after July 2007 to ensure stability close to Cambridge Bay (Canadian Arctic Archipelago).

2.1.4 Sea-ice models

Within NEMO3.1 the ocean is interfaced with the Louvain-La-Neuve sea-ice model version 2 (LIM2, Fichefet and Maqueda, 1997), or version 3 (LIM3, not tested here; Vancoppenolle et al., 2009b, a).
130 However here we also use another community sea-ice model, CICE (described below).

LIM2 is a simple one-category ice model based on a Semtner 3-layer thermodynamic model (two layers of ice and one layer of snow). A Viscous-Plastic (VP) constitutive law relates the internal ice stresses to the strain rates and the ice strength. It is based on an elliptical yield curve and a normal flow rule (Hibler, 1979). The VP solution is approached by iteration of a relaxation
135 scheme to the implicit ice velocity problem. LIM2 was used for the first two hindcasts (details given below in Section 3.1 and Table 1) for sanity checks relative to the configuration used in ORCA12-T321. The latter actually used an upgraded dynamic solver based on the Elastic-VP (EVP) approach (Hunke and Dukowicz, 1997, 2002; Bouillon et al., 2009) instead of the VP solver described above.

CICE (Hunke, 2001; Lipscomb et al., 2007; Hunke and Lipscomb, 2010) is a dynamic/thermodynamic
140 sea ice model, which can be used as a stand-alone model or coupled to an ocean model inside a climate modelling system. Herein, it is coupled to NEMO on the same grid as a single executable (Hewitt et al., 2011). CICE calculates the evolution of a thickness distribution. The thickness distribution evolves with both thermodynamic (vertical growth/melt, new ice formation and lateral melt) and dynamic processes (advection and redistribution). The momentum equation is solved with
145 the same EVP approach as described above for LIM2-EVP, although on a slightly different stencil (Arakawa C-grid in LIM2-EVP and B-grid for CICE). LIM2-VP is discretized over a B-grid stencil.

In both sea-ice models, the ice is supposed to be "levitating" (following the convention of Campin et al., 2008) over the ocean, that is, the growth or melt of ice is not impacting the ocean volume nor the presence of ice is impacting the position of the ocean surface. However, the ocean surface salinity
150 needs to evolve appropriately during brine rejection or the flushing of melt water. For this, a virtual salt flux approach is used, which converts the freshwater flux into a salinity flux to represent dilution or concentration of salt at fixed water volume.

2.1.5 LIM2 and CICE parameters

LIM2 solves the VP dynamics with prescribed ice-water and air-ice drag coefficients. The momentum stress is expressed using a simple quadratic law (McPhee, 1975) with a 0° turning angle for
155 both air and ocean in contact with ice. In the ORCA12-T321 run of Mercator-Océan, the air-ice drag was reduced to 1.5×10^{-3} , whereas the default value of 1.63×10^{-3} is used in our CREG12 LIM2 runs. The ice-water drag is fixed to 1×10^{-2} in all LIM2 runs (including as in the Mercator-Océan run). In ORCA12-T321, the ice module is called with a time-step of 720 s (every two ocean model

160 time-steps), the EVP solver uses 400 sub-timesteps and a damping elastic time of 1350 s. In the CREG12 LIM2 runs, the ice model is called every 5 ocean time-steps (equivalent to an ice time-step of 1800 s). The VP solver performs 20 outer loops (the default is 2) with a linear residual at convergence of 1×10^{-6} or a maximum of 550 iterations. It should be noted here that NEMO-LIM2 users can tune the total ice extent and volume by adjusting the parameter `hiccrit` (Wang et al., 2010),
165 a characteristic thickness that is used to determine changes in open water area during ice growth. Nonetheless, overestimation of the total ice extent, or volume is often reported in NEMO-related publications (Massonnet et al., 2011; Blockley et al., 2014), likely related to the use of a too large value of the aforementioned parameter, for given configuration and forcing. ORCA12-T321 used `hiccrit`=0.6 m and the same value is applied in the CREG12 LIM2 runs.

170 In CICE, both air-ice and ocean-ice stresses are also expressed using a simple quadratic law with a 0° turning angle. Following Roy et al. (2015) for our last two hindcasts and since our first ocean layer thickness is relatively small, the ice-ocean drag coefficient is computed by a log-layer assumption using the oceanic first layer thickness and a roughness length scale of 0.03 m as suggested by Maykut and McPhee (1995) which yields a drag coefficient of 2.32×10^{-2} . The air-ice stress
175 involves a more sophisticated formulation that takes into account the stability of the atmospheric boundary layer. Following again Roy et al. (2015), the roughness length scale for ice surface is set in our latest run to the value used in the Canadian Global Re-Forecast (CGRF, Smith et al., 2014) for consistency between the ice-air stress computed in CGRF and in CICE. These modifications can be seen as a more objective way of deriving the drag coefficients, as they are not retrieved from a
180 calibration exercise.

Ten thickness categories are defined in CICE (as in Smith et al., 2015), with specific representation of both thin ice and thick ridged ice. CICE is called at every ocean time-step. The remapping advection scheme is used and the EVP solver is run with 920 sub-timesteps. The ice strength is computed using the more physically realistic approach of Rothrock (1975). Based on studies with
185 CICE run offline (Lemieux et al., 2015a), we increase the value of the newly formed ice in CICE (`hfrazilmin`) from 5 cm to 8 cm. Otherwise, the default parameters and parametrizations of CICE thermodynamics were used with no further tuning. The number of layers is set to the default value (four ice layers and one for the snow). The default Community Climate System Model 3.0 scheme (CCSM3; Vertenstein et al., 2004) is used to calculate the albedo and the attenuation of the
190 absorbed shortwave radiation. The sea-ice is assumed to have a salinity of 3.2 g/kg. Lateral melting depends on a specified value of the average diameter of the ice floes (Steele, 1992) which is kept to the default value of 300 m.

2.2 Model input data

2.2.1 Atmospheric forcing

195 The model is forced at the surface using the CGRF product (Smith et al., 2014) from 2002 (2003 for some other runs) to 2009. This product consists of a series of re-forecasts using available historical operational analyses from the Canadian Meteorological Centre of Environment Canada. As such, it is not a true reanalysis as other centres produce. However, because it uses the global Canadian Numerical Weather Prediction (NWP) model (last updated in 2011), it provides a consistent set of
200 global forecasts at higher resolution (nominally 33 km at 60°N) than typical reanalyses. The only source of variation in the quality of the reforecasts is the quality of the initial state (the analysis), which varies during the historical period with the assimilation method and volume of observations used (more details can be found in Bélair et al., 2009). The resolution offered by this product allows for better resolution of mesoscale atmospheric features. The short and long wave radiation fields
205 however require some level of correction as the NWP model is unable to simulate with sufficient accuracy the marine clouds. A climatological correction based on the month of interest but also on the forecast hour is derived from the GEWEX (https://eosweb.larc.nasa.gov/project/srb/srb_table) radiation product.

The frequency of the forcing fields is set to 3 hours, using hours 6-27 of each CGRF initiated at
210 00 UTC. CGRF is provided on 10-m wind and 2-m thermodynamic levels. Those are not true "prognostic" model levels but since conventions and model output dissemination requires these levels, a "diagnostic" procedure is used to derive quantities there. The first prognostic level for wind and temperature in CGRF is in fact approximately at 40 m, and quantities at this level are also available and are thought to be less dependent on assimilated surface conditions and approximations made
215 during the diagnostic procedure. We have therefore used the product at this level as input to the CORE air-sea exchange bulk formulae and the equivalent in CICE. The only limitation to this approach is in LIM2, where input atmospheric conditions are assumed at 10 m with pre-set constant neutral coefficients, causing an over-estimation of wind-stress by approximately 20% to 50% (the same overestimation problem likely affects the calculation of turbulent heat exchanges.)

220 2.2.2 Bathymetry, initial and lateral boundary conditions

The bathymetry used in the CREG12 configuration is taken from that used in the ORCA12-T321 run of Mercator-Océan. It is based on ETOPO2 (<http://www.ngdc.noaa.gov/mgg/global>, Amante and Eakins, 2009). The minimum depth is set at 20 m.

Two sets of initial ocean conditions (comprising 3D velocities, temperature, salinity and sea surface height) have been used. Firstly a reanalysis product, GLORYS2v1 (Ferry et al., 2012) is used.
225 This covers the satellite-altimetry and ARGO period (1993-2010), with assimilation of both of these datasets in the reanalysis as well as other in-situ data. However we found that, although the assim-

ilation of observations leads to a remarkable agreement with observations at lower latitudes, GLO-
RYS2v1 suffers from serious departures relative to observations and to the Polar Science Center Hy-
drographic Climatology (PHC, http://psc.apl.washington.edu/nonwp_projects/PHC/Climatology.html)
in the Arctic¹. The second set of initial conditions used is simply derived from the ORCA12-T321
run of Mercator-Océan, which has better hydrographic properties in the Arctic Ocean but is not as
accurate as GLORYS2v1 at lower latitudes.

Sea ice initial conditions are taken from the same initial condition product, that is either GLO-
RYS2v1 or ORCA12-T321, which use the mono-category LIM2 model. The ice concentration and
ice thickness of these products are applied to the corresponding ice category in CICE, the other cate-
gories remaining empty. It then takes several month of simulations before a realistic ice distribution
can be recovered. An initial spread among several categories would therefore be more realistic. For
snow, the ice category that receives the ice volume also receives the snow volume present in the
initial conditions.

Along the lateral open boundaries, time-evolving monthly conditions (comprising 3D velocities,
temperature and salinity from 2002 to 2009) are taken from the same products as the initial con-
ditions. More specifically, a clamped velocity condition is specified (hence lateral transport) and a
radiation scheme following the advective characteristic is applied for temperature and salinity com-
bined with restoring to input values. The restoring time is 15 days when radiating outward and 1 day
when inward. A closed wall boundary condition is applied to sea ice in LIM2 and CICE.

The river freshwater discharge was taken as in T321 from the monthly climatology of Dai and Trenberth
(2002). No attempt was made in these hindcasts to investigate the impact of the interannual variation
of Arctic river or glacial discharge, which was left to a future study.

2.3 Verification package

Evaluation of the system is performed by comparing model outputs with ocean observations. Addi-
tionally, the model outputs are compared with other model estimates and with climatologies. During
the development phase, with the model running in hindcast mode, this evaluation provides an assess-
ment of the improvements introduced with each change to the model configuration. Once the forecast
system is operational, the verification package will provide an assessment of forecast accuracy.

The CONCEPTS evaluation strategy defines a set of model output fields, a database of ocean ob-
servations from both in-situ and remote sensing measurements, and a suite of metrics for comparing
the two. This approach has been designed for the CREG12 configuration, but was developed in such
a way that it can easily be transferred to other CONCEPTS systems. The key model outputs for eval-
uation are sea surface height, ocean temperature, salinity and velocity, and sea ice thickness, concen-

¹ Among other poor characteristics, the doming of sea surface height in the Beaufort Sea is absent and the Atlantic layer
apparently spreads anti-cyclonically instead of cyclonically. This is in apparent contrast to studies done using GLORYS1,
which were more successful, such as in Lique et al. (2011)

tration and velocity. Additional derived output fields include transports through sections, freshwater content and mixed layer depth. The observation database incorporates measurements included in existing global databases, combined with data from individual observation missions. These include missions using new technologies developed to provide measurements in the ice-covered regions of the Arctic. The ocean observation database includes traditional ship-deployed and moored in-situ measurements of temperature, salinity and velocity, together with measurements from ARGO drifting profilers, ice-tethered profilers, gliders, mammal-mounted instruments and satellite remote sensing. The sea ice observations include thickness and drift measurements from ice mass balance buoys and upward-looking sonar together with remote sensing from aircraft- and satellite-mounted instruments.

3 Model simulations and evaluation

3.1 Simulations

Five hindcast simulations, H01 to H05, are carried out covering the years 2003 to 2009, and these are briefly described in Table 1. LIM2 is used in H01 and H02, and CICE in H03 and higher. H01 is initialized from GLORYS2v1, which is found less reliable than ORCA12-T321 in the Arctic Ocean, our focus region. Hence H02 and higher are started instead from ORCA12-T321. Changes related to air-ice and ocean-ice drags based on Roy et al. (2015) were incrementally implemented in H03 to H05. Parameters are defined in Section 2.1.5. Hence H02 uses for instance a lower ocean-ice drag coefficient relative to H05 (approximately half). The treatment of the air-ice stress is also noteworthy different in H02 as explained in Section 2.2.1, and therefore the magnitude of the stress is over-estimated relative to H05. For the interest of the reader, we also note that the latest hindcast H05 has been used in a study of the role of eddy-induced transport of heat and buoyancy in the Labrador Sea (Saenko et al., 2014).

3.2 Hydrography and circulation evaluation

The focus of the evaluation is the most-recent model run, H05, but there are some brief comparisons with the earlier H02, which incorporates the LIM2 ice model rather than the CICE model. In this sense and in spite of other differences, H02 is the closest simulation to the ORCA12-T321 run. Most of the comparisons presented here are for the mean fields for the period 2003–2009 with additional discussions on time variability.

3.2.1 Sea surface height

Satellite altimeters provide a continuous record of sea surface height (SSH) anomalies since 1993 (Benveniste, 2011), with accuracy at the cm level. Figure 3 shows the mean (top), standard deviation (middle) and skewness (bottom) of SSH for the North Atlantic for the period 2003–2009 from

the model hindcast H05 (left panels) and from the satellite record. The altimeter estimates of the standard deviation and skewness are produced using the gridded $1/4^\circ$ SSH [AVISO](http://www.aviso.oceanobs.com/en/data/products/auxiliary-products/mss/index.html) anomaly product distributed by Archiving, Validation and Interpretation of Satellite Oceanographic data (AVISO, <http://www.aviso.oceanobs.com/en/data/products/auxiliary-products/mss/index.html>). The mean altimeter SSH is the sum of the 2003–2009 SSH anomalies and the CNES–CLS09 Mean Dynamic Topography (MDT, Rio et al., 2011).

The mean SSH fields from the model and altimeter record are very similar. The sharp gradient of the Gulf Stream can be seen in both, leaving the coast of North America around 35°N , and following a similar path eastwards. The high SSH of the subtropical gyre can be seen to the south of the Gulf Stream, and the low SSH of the subpolar gyre to the north. The model estimate shows some sharper gradients, for example along the Labrador coast, but this is likely because of the higher horizontal resolution of the model ($1/12^\circ$) compared with the resolution of the altimeter product ($1/4^\circ$).

The spatial distribution of the magnitude of SSH variability, represented by the standard deviation plots, shows good agreement between the model and the altimeter measurements. The altimeter data shows in general though a broader structure of medium values of standard deviation to the south of Gulf Stream whereas that of the model shows medium values extending along the path of the North Atlantic Current.

Positive and negative skewness corresponds to the meandering of a free jet such as the Gulf Stream or the variability caused by warm- and cold-core eddies (Thompson and Demirov, 2006). Typically, the zero contour of skewness separating strong regions of negative and positive skewness is a good indicator of the centre position of the mean currents. There is again good agreement between the model and the altimeter record in terms of the distribution of skewness for the Gulf Stream area, with the zero contour of the model being positioned slightly more to the north. A broad region of negative skewness in the model is also clearly visible in the mid to eastern Atlantic Ocean which is not seen in the altimeter data. The interpretation of this is more difficult, except to note that the model must be producing more intense cyclonic than anticyclonic deviations in this region. Finally, the zero contour helps to define the position of the Azores Current, which is well reproduced in the model in general but with perhaps a slightly more intense and narrower jet.

Most of the satellite altimeters that contribute to the AVISO record are unable to produce useful estimates of SSH in the Arctic, either because their orbits do not extend far enough north or because sea ice prevents the altimeter signal reaching the sea surface. However Farrell et al. (2012) used measurements from the ICESat and Envisat satellite missions to create an Arctic MDT for the period from 2003 to 2009, corresponding ~~with~~^{to} the period of the hindcast. This resolves the large (basin) scale features of the MDT, although it is unable to resolve small-scale features. Figure 4 shows the mean Arctic SSH from H05 and the MDT of Farrell et al. (2012). There is good agreement between the two estimates, both in terms of the patterns of SSH and the SSH gradients. For example H05 shows a cross-Arctic sea level difference, from the high of the Beaufort Gyre to the low north of

Spitzbergen, of approximately 60 cm compared with a difference of about 65 cm in the MDT of Farrell et al. (2012). Kwok and Morison (2011) similarly use ICESat data (winter only) to estimate the MDT of the Arctic, including its variability. The interannual variability of mean SSH in H05 (not shown here) compares well with their estimates, particularly in the Canada Basin.

335 3.2.2 Surface circulation

Figure 5 compares the mean current speeds from hindcast H05 to a $1/2^\circ$ resolution climatology derived from near-surface drifter velocity estimates (Lumpkin and Johnson, 2013). The model speeds at 15 m depth (corresponding with the depth of the drifter drogues) were averaged for the period 2003–2009 and regridded at the same $1/2^\circ$ resolution as the climatology. The drifter estimates typi-
 340 cally have an estimated error less than 3 cm s^{-1} in the deep North Atlantic. The general agreement between the model and drifter climatology is good; for example, the estimates of the speed and the position of the Gulf Stream and the North Atlantic Current appear similar. On the north flank of the Gulf Stream, a weak but persistent branching is clearly visible in both plots, east of 70°W , although that of the model detaches from and rejoins the Gulf Stream a little too early. This secondary current
 345 system is likely related to the Slope Water Current described in Pickart et al. (1999) and Dupont et al. (2006). The East and West Greenland currents, and the Labrador Current, contain more details in the model than can be captured by the drifter resolution, but the separation of coastal and shelf jets is in good agreement with other observations (e.g., Higginson et al., 2011). Again, the path of the Azores Current is visible in both model and observations.

350 3.2.3 Temperature and salinity

Quality-controlled measurements of ocean temperature and salinity (TS) are available from the global CORA3.4 database distributed by MyOcean (www.myocean.eu). This database includes measurements from ship-based surveys, moorings and the drifting profilers of the ARGO network. In the Arctic there are relatively few observations compared with other ocean basins. Whilst some Arctic
 355 observation programmes have been incorporated into the CORA3.4 database, others are not yet included. We have undertaken a search of data available from all programmes, and combined them with the CORA3.4 observations where they are missing. These observation programmes include the Beaufort Gyre Exploration Project (BGEP, <http://www.whoi.edu/page.do?pid=66296>), the Ice–Tethered Profiler project (ITP, <http://www.whoi.edu/page.do?pid=20756>), the Canadian Basin Ob-
 360 servational System (CABOS, <http://nabos.iarc.uaf.edu/index.php>), the Switchyard project (<http://psc.apl.washington.edu/switchyard/>), the North Pole Environmental Observatory (NPEO, <http://psc.apl.washington.edu/northpole/>), and monitoring programmes in Davis Strait (e.g., Curry et al., 2013), Barrow Strait (e.g., Hamilton et al., 2013) and Fram Strait (e.g., Schauer et al., 2008).

Figure 6 shows the mean TS bias for hindcast H05 for the period 2003–2009. Model values are
 365 extracted at the same time and location as observations, and the bias is calculated as the model esti-

mate minus the observation. The biases are averaged in 1 degree bins for the top 200 m, and between 200 m and 500 m depth. These intervals are chosen to quantify the near-surface (including shelf) and intermediate depth anomalies. Measurement errors are negligible (typically $\pm 0.01^\circ\text{C}$ for temperature and ± 0.01 for salinity e.g., Talley et al., 2011). However the model output is grid-cell averaged
370 whereas the observations are point measurements that will be subject to additional variability. Accordingly, we consider averaged biases rather than comparisons with individual measurements.

Over large areas of both the North Atlantic and the Arctic oceans the average temperature biases are less than $\pm 1^\circ\text{C}$ and the salinity biases are less than ± 0.5 . However, a warm and salty bias is seen in the central North Atlantic and in the currents that form the subpolar gyre. This bias is strongest in
375 the surface layers, averaging more than 2°C and 0.75 in some places, and extends into the Iceland and Norwegian seas. The temperature bias extends southwards along the path of the Gulf Stream, particularly in the surface layers. A cold bias also extends from the north side of the Gulf Stream toward the coast of the US and Canada. The salinity bias is largest in the Labrador Current. A salty bias is seen in the upper layers of the Beaufort Sea, extending along the coast of Canada toward
380 Fram Strait (see also Section 3.2.4). Conversely, the waters in the centre of the Greenland-Iceland-Norwegian Seas are colder and fresher.

The vertical structure of the model TS compared to observations is shown in Figure 7. Four domains were chosen to represent regions of oceanographic interest (the subtropical and subpolar gyres, the Beaufort Gyre and the Nordic seas). These domains (except for the subtropical gyre) correspond with regions of relatively high temperature or salinity averaged biases identified in Figure 6.
385 For each domain all available observations were averaged to give single temperature and salinity profiles. Model outputs at the same times and locations were extracted from hindcast H05, and also from the GLORYS2v3 reanalysis product (Ferry et al., 2012) and from the Polar Science Center Hydrographic Climatology (PHC). These were similarly averaged across each domain to give single
390 temperature and salinity profiles for each product in each domain.

The profiles for the subtropical gyre domain (box d) show that the model does a good job of representing both temperature and salinity, although the top ocean layers are too fresh by 0.5. In the subpolar gyre domain (box c) the model bias in salinity is positive, with a maximum of less than 0.5 around 100 m depth. The warm bias has a maximum of around 2°C at a similar depth. In the
395 Greenland and Norwegian seas (box b), there is a fresh and cold bias, restricted to the top 100 m of the ocean. In the Beaufort Sea (box a) the temperature biases are small (less than 0.5°C), but the profile shows the bias to be cold in the Atlantic water layer (around 500 m depth) and near the surface, and slightly warm in the Pacific water layer (around 150 m depth, Steele et al., 2004). The vertical temperature structure is not well reproduced by the model. This suggests that there may be
400 problems with the transport and transformation of Pacific waters in the model, and this is an area for further investigation. We can only tell at this point that Pacific water signature weakens with time in H05 (not shown). A salty bias in the Beaufort Sea is restricted to the upper 75 m of the water

column. Note that GLORYS2v3 and PHC are in good agreement for temperature but both depart ~~considerably~~ noticeably from the observations in this area.

Examining the Beaufort Sea salinity bias in a little more detail, Figure 8 shows the mean liquid freshwater content equivalent depth for the Arctic from H05 and from PHC. The freshwater content is calculated using the method described in Proshutinsky et al. (2009), with a reference salinity of 34.8. There is good agreement in terms of the distribution of liquid freshwater, with the greatest concentration in the Beaufort Gyre, but the total modelled freshwater content in the gyre is greater than in the climatology. This is likely because the PHC does not incorporate observations beyond 1998 and therefore does not reflect the recent increase in freshwater content estimated by Proshutinsky et al. (2009). In order to investigate whether this increase is reproduced in the different simulations, we average the total monthly modelled liquid freshwater content over a pre-defined region of the Beaufort Gyre. We compare the modelled totals (H02, H05 and ORCA12-T321) to the summer estimate (and uncertainties) over the same region based on observational data (Proshutinsky et al., 2009, and updates by pers. comm. of A. Proshutinsky, 2013) in Figure 9. Because the modelled totals are plotted as monthly values, they exhibit a seasonal cycle that the observed estimate based on summer campaigns ~~can not. The estimate uncertainty is about 9~~ cannot reproduce. Based on the uncertainties provided with the summer estimate, we concluded that the observational error in total freshwater content is about 10%. The two CREG12-based hindcasts reproduce fairly realistically the observed increase in freshwater content (although tapering by the end of the simulation period) whereas the ORCA12-T321 content exhibits no such increase. We partly attribute this discrepancy to differences in atmospheric forcing products used in our hindcasts and ORCA12-T321. The fact that H05 shows a slightly poorer agreement with the observed freshwater estimates than H02 by the end of the simulation is due to the weaker Ekman pumping in the Beaufort Gyre, the latter explained by the smaller roughness and associated ice-air drag as described in Section 2.1.5 and Table 1. This will be illustrated from a different point of view in Section 3.3.2.

3.2.4 Sections across Fram Strait and Davis Strait

Arrays of moorings have been deployed across the main pathways for exchange of water between the Arctic and Atlantic, for example in Fram Strait (Schauer et al., 2008) and in Davis Strait (Curry et al., 2013). Figures 10 and 11 show a comparison of mean temperature, salinity and velocity estimated from these observations with corresponding estimates from hindcast H05 for Fram Strait and Davis Strait respectively. The Fram Strait mooring observations cover the period 2005–2009, and the Davis Strait moorings cover 2004–2009, although not all instruments were deployed for the whole period. For each instrument all available observations are averaged. The output from hindcast H05 is averaged for the corresponding times ~~for~~ of each instrument. The contribution of measurement errors and mesoscale variability is negligible because of instrument calibration and averaging. However sampling uncertainty may be an issue in the central sections of the straits where the moorings are spaced

further apart, especially in Fram Strait where there is a recirculation within the Strait (Schauer et al.,
440 2004).

Overall there is good agreement between the model and observations in Fram Strait. The large velocity of the northward-flowing West Spitzbergen Current and the southward-flowing East Greenland Current are very similar in magnitude and location. The temperature and salinity structure of the two currents is broadly similar, although the model shows a cold bias in the central channel and
445 the modelled northward-flowing water close to Spitzbergen is a little saltier than observed. The observations show a weaker northward-flowing branch of the West Spitzbergen Current in the central channel, as described by Schauer et al. (2004), but this is absent in the simulation. This may explain the cold bias in the modelled near-surface waters in the centre of the strait.

In Davis Strait the observed and modelled temperatures are in good agreement. The salinity fields
450 are also generally good, and the velocity maxima of the northward-flowing West Greenland Current and the southward-flowing Baffin Island Current (BIC) are similar in magnitude. However, the northward-flowing water on the Greenland shelf is a little too salty, likely related to the salty bias in the subpolar gyre described earlier, and the BIC is displaced further offshore in the model. There does not seem to be a strong temperature or salinity bias in the Arctic outflows through either Fram
455 Strait or Davis Strait, suggesting that this is not the source of the biases seen in the Atlantic and discussed in the previous section.

The mean net liquid volume transport for 2003–2009 in hindcast H05 for Fram Strait is 2.7 Sv (1 Sv is $10^6 \text{ m}^3 \text{ s}^{-1}$) toward the south, compared with an observational estimate of 2 ± 2.7 Sv (Schauer et al., 2008). For Davis Strait the model mean liquid volume transport is 1.9 Sv toward the south, compared
460 with an observed 1.6 ± 0.5 Sv (Curry et al., 2013). The large observational uncertainties are generally associated with interpolation between mooring locations rather than measurement errors (see, for example, Fährbach et al., 2001).

3.3 Sea-ice evaluation

3.3.1 Ice concentration, thickness and volume

465 Estimates of the total ice extent (where ice concentration is higher than 15%) have been derived from satellite products at the National Snow and Ice Data Center (NSIDC, Cavalieri et al., 1996, updated 2008), filling the North Pole data hole with 95% ice concentration. Ice extent is a more robust metric than ice area in summer as the latter is biased due to melt ponds detected as open water with errors on average around 10% (Comiso et al., 1997). Comparing H02 and H05, the implementation of CICE
470 in H05 is beneficial in terms of better reproducing the seasonal cycle (Figure 12, top panel). The ice thickness distribution allows for larger rates of melting and growth in the small ice thickness categories, thus enhancing the seasonal cycle of ice extent and bringing it closer to observations. Due the missing North Pacific Ocean in the CREG12 domain, the maximum winter extent in the

hindcasts does not reproduce the NSIDC estimate which covers all northern hemisphere (to ease
 475 ~~data-exchange-and~~ comparison, ORCA12-T321 ~~was provided too~~ output is considered only on the
 CREG12 grid domain). In terms of interannual variability, looking at September ice extent (Figure 12,
 bottom panel), H05 ice loss is faster than H02 at the beginning of the simulation (2003-2005), indi-
 cating an initial imbalance in thermodynamics mainly in H05 which necessitates close to two years
 to be resolved (see Section 2.2.2 for the initialization of CICE). After this, the total ice extent in H05
 480 stays close to the observed estimate between 2005 and 2009. H05 September ice extent then starts to
 depart from observations after 2010 due to an anomalous accumulation of ice in the Beaufort Gyre
 and retreat elsewhere. H02 and T321 have a too large September ice extent but the negative trend is in
 general closer to observations than in H05, even though the period for comparison is too short to be
statistically significant. This can be related to the fact that both H02 and ORCA12-T321 are in better
 485 thermodynamic balance with the initial condition, which itself is derived from a simulation using
 LIM2, than H05 which goes through a two-year adjustment period. The 2007 minimum is well re-
 produced by H05 in terms of total ice extent, although the regional structure shows differences from
 the observations (Figure 13). The ice concentration in Beaufort and Chukchi Seas is a little too high
 and that in the tongue of ice connecting the central pack along the Severnaya Zemlya Archipelago
 490 to the mainland is somewhat too low. The ORCA12-T321 and H02 ice concentration fields are very
 similar in spatial structure, with T321 showing a sharper transition at the ice pack edge. They both
 overestimate the ice concentration in the Beaufort Sea and in the East Siberian sector, in agreement
 with the total ice extent results.

In-situ ice thickness observations are available from a number of different sources. Ice mass bal-
 495 ance buoys (e.g., Polashenski et al., 2011) drift with the ice, measuring the evolution of the ice
 thickness with ± 0.01 m precision. For practical reasons, the deployments are generally in areas
 of multi-year ice. As we concentrate on the Central Arctic, this is less of a concern since the
 multi-year ice is the most representative type in this area. Sub-sampling is however still an issue
 and we therefore concentrate on the large structures. Figure 14 shows the mean difference be-
 500 tween the model sea ice thickness and the measured thickness. For each observation, the model
 thickness at the same time and location is obtained, and a bias calculated. Biases are binned into
 boxes approximately 100 km square, and averaged. H05, which uses the CICE ice model, clearly
 produces a result closer to observations than H02, which uses LIM2, but the ice in the Beau-
 fort Gyre is still too thick. Upward-Looking Sonars (ULS) have been deployed on a number of
 505 subsurface moorings, providing high frequency measurement of the ice draft from beneath. This
 data can be used to produce an estimate of the thickness distribution at the mooring location with
 an accuracy of ± 0.1 m (Kwok et al., 2004), which can be compared with the ice thickness dis-
 tribution from the CICE model. Figure 15 compares the estimates from H05 with observations
 at one of the BGEP moorings (<http://www.whoi.edu/beaufortgyre/data>) and at the NPEO moor-
 510 ing (<http://psc.apl.washington.edu/northpole/>, Morison et al., 2002). The BGEP mooring data was

averaged for the period September 2003 to December 2009. The NPEO mooring data was for the period January 2003 to December 2009 (but there are some gaps in the record). In each case the model output is averaged for the same period as the observations. The model reproduces the thickness distribution at both sites quite well, although it tends to overestimate the thicker ice categories in the Beaufort Gyre and underestimate them near the North Pole. Conversely, it can be noted that thinner categories are underestimated in the Beaufort Gyre but overestimated near the pole.

The spatial structure of the ice mean thickness (local total ice volume divided by total ice concentration) is also compared to estimates from the ICESat mission (Kwok et al., 2009) ~~for the period October-November 2007~~. The uncertainty associated with the ICESat estimate can be as large as 0.5 m. Thus, we only concentrate on the broad patterns. Figure 16 shows that ORCA12-T321 and H02 (both of which use LIM2) overestimate thickness over a large area. The mean ice thickness in H05 is closer to the ICESat observations, but there is a region of overestimated thickness in the Beaufort Gyre and an underestimation elsewhere which is consistent with our findings from the ice mass balance and ULS measurements, and also with results of Roy et al. (2015).

Finally, the domain total ice volume of the different model simulations is compared to the estimate of the data-assimilative model PIOMAS (Zhang and Rothrock, 2003). This model ice volume compares well with estimates from ICESat and CryoSat2 (Laxon et al., 2013) and is therefore deemed a reasonable reference ~~The error bars are not known but could be up to 25%~~ ~~with a 10-15% uncertainty (based on their figure 3)~~. The seasonal cycle (Figure 17, top panel) for H05 is very close to the PIOMAS value, and a clear improvement over H02 and ORCA12-T321. The September values (Figure 17, bottom panel) emphasize the discrepancy between the different hindcasts: H05 is close to PIOMAS in magnitude and trend (although with a ~~one-month~~ ~~one-month~~ lag), while ORCA12-T321 and H02 do not have a clear trend and the volume is overestimated by 50 to 100%. This volume overestimation in ORCA12-T321 and H02 is consistent with the findings from in-situ and satellite thickness measurements. Here too, the different drag coefficients partially explained the convergence and accumulation of ice in the Beaufort Gyre. The higher ice-ocean drag and the lower air-ice drag in H05 both concur to reduce the ice velocity and therefore the Ekman convergence there, relative to H02.

The modification to the surface ice roughness between H04 and H05 has a positive impact, improving the absolute value and trend in the volume (not shown). However, although the total volume of H05 is very much on par with estimates from PIOMAS, this conceals regional errors such as an overestimation of ice thickness in the Beaufort Gyre that were discussed earlier. The source of these errors in the Beaufort Gyre is likely related to the ice drift pattern, discussed in the following section.

3.3.2 Ice ~~drift~~velocity

~~Ice drifts for March 2003-2008 are compared~~ ~~Satellite estimates of mean ice velocity, produced at 25 km resolution~~ (Fowler et al., 2013), ~~were obtained for March in the years 2003 to satellite estimates from (source: NSIDC) 2008 from NSIDC. These are averaged and compared to averages~~

for the corresponding period from the same three hindcasts (ORCA12-T321, H02 and H05) in Figure 18 at 25 km resolution and observations from ice buoys deployed as part of the International Arctic Buoy Program (IABP; <http://iabp.apl.washington.edu/>). The satellite and model estimates are coherent over large spatial scales (500 km), with a clearly defined Beaufort Gyre, Transpolar Drift, and Fram Strait outflow. The estimates differ mainly in the intensity of the ice flow in the Beaufort Gyre and the Transpolar Drift. One can see the improvement from hindcast H02 to H05 as the ice-water and air-ice drags are adjusted following a semi-objective approach (Roy et al., 2015). However, the ice drift velocity in H05 is still overestimated. In the too high compared to the satellite estimate. The ORCA12-T321 solution, the air-ice drag is slightly decreased and actually yields the best modelled velocity fields, is the closest to the satellite estimate.

Given the similarity in ice circulation between the different products, a simple metric is now considered, the averaged ice drift bias relative to the IABP buoys over the 2003–2009 period (Figure 19). The difference between the velocity calculated from the buoy displacements of the International Arctic Buoy Program (IABP; <http://iabp.apl.washington.edu/>) and from the model at corresponding times and locations is averaged for the period 2003–2009 (Figure 19). The Pathfinder gridded estimates are buoy locations are provided with an uncertainty of ± 100 m so, assuming an monthly averaged velocity of 0.05 m/s, the uncertainty is less than 1%. The monthly ice velocity field is generally coherent over large scales, so the issue of irregular sampling by the buoys should not be too critical. Figure 19 shows that the satellite estimate is the closest to buoy drifts (albeit with a slight negative bias), followed by ORCA12-T321 and H05 and H02. The H05 bias is close to that of ORCA12-T321 but starts to deviate in late 2006. H02 has the largest bias. Hence, the averaged bias confirms the visual examination of the mean March circulation. These results are consistent with those from the average March velocity maps in Figure 18.

This evidence suggests that Ekman transport is still acting too strongly in H05, driving a convergence of ice and accumulation of multi-year ice in the Beaufort Gyre. An obvious reasoning is that the air-ice stress is too large (either due to too strong winds or/and drag coefficient), driving the ice too fast. However, the CGRF surface winds tend to show a weak negative bias compared to observations at Ice Station Tara (not shown). This is in contrast to some reanalysis products compared by Jakobson et al. (2012) such as ERA-INT. Moreover, the surface ice roughness lengthscale in CGRF is actually smaller than the one used in ERA-INT. Hence the air-ice stress is less likely to be overestimated. On the other hand, the freshwater content increase during the period 2003–2009 in H05 is slightly weaker than observed (Figure 9), which suggests the opposite, that is, the convergence of freshwater due to Ekman transport acting on the ocean may be underestimated. This issue needs to be further studied. Some mechanisms explaining variations in the Arctic freshwater content caused by dependencies on model parameters are also assessed in Roy et al. (2015). Preliminary results point to deficiencies in the vertical mixing scheme used in H05 ($k - \epsilon$) in the Arctic upper ocean

which would explain the overly strong ice ~~drift~~-velocity in the Beaufort Gyre by underestimating the shallow convection under the ice.

585 Additionally, we note that the lack of landfast ice parametrization may explain the over-estimation of the ice ~~drift~~-velocity in all model runs in the East Siberian, Laptev and Kara Seas in Fig. 18.

4 Conclusions

The development of a high resolution ice-ocean modelling system is a challenging task that requires a team effort. In CONCEPTS this is achieved by collaborations among different Canadian gov-
590 ernment departments and international collaborators such as Mercator Océan. The CREG12-based system consists of state-of-the-art ocean and sea-ice models, a comprehensive verification package, and a data assimilation capability under development. Before proposing the system for operational implementation, the capability of the ice-ocean model to produce high-quality hindcasts must be demonstrated. Hence, the present approach of producing a series of hindcasts and by identifying
595 deficiencies, helps in deciding which aspects of the system need to be improved. For instance, the upper ocean physics and more accurate initialization fields appear as areas of particular concern.

Each multi-year hindcast, driven by the high-resolution CGRF forcing, shows incremental improvements with changes to the initial and boundary conditions, the lateral friction schemes, turbulent mixing parametrizations, and finally the change of sea-ice model from LIM2 to CICE. The
600 verification package includes a variety of ocean and sea-ice observations. It demonstrates the capability of the model in hindcasting the mean, variance and skewness of the SSH, the position and strength of the surface circulation.

In terms of temperature-salinity distributions, the initial conditions (however accurate or poor they can be) still imprint the results after 8 years and therefore only variations in the upper ocean can be
605 analyzed. From this point of view, the $k - \epsilon$ mixing scheme seems adequate in the north Atlantic but likely underestimates the shallow convection below the ice and this may explain the degradation of some of the upper ocean water masses of the Arctic Ocean such as the Pacific Layer. Nonetheless, the freshwater content in the Beaufort Sea and its interannual variations are well reproduced by the model, including the seasonal and interannual variations of the Arctic sea-ice extent and total
610 volume. The Fram Strait long term averages were in general well reproduced by the model, with the exception that the model misses the offshore extension of the northward flowing branch of the Spitzbergen current, which leads to a small but still important loss of Atlantic inflow into the Arctic. The Davis Strait results show that the model has a northward Western Greenland Current flowing a little too far north and a too strong southward Baffin Current, the net being too much Arctic
615 southward flow, while the modelled structure is generally accurate.

The model reproduces the major patterns of sea-ice ~~drift~~-velocity but the intensity is too strong, especially in the Beaufort Gyre. This is correlated to too thick ice in the Beaufort Sea (and too thin

over the pole) which points to an overestimated Ekman transport in the upper ocean but needs to be further investigated. Preliminary results suggest –again– deficiencies of the $k-\epsilon$ mixing scheme during winter convection. The change from LIM2 to CICE was beneficial in terms of thermodynamics as the seasonal cycle of total ice extent and volume is more pronounced and closer to observations and qualified modelled estimates, but other differences between the two, such as the ice drift-velocity intensity and ice convergence in the Beaufort Gyre are related to differences in the drag coefficients. No effort was made for instance to improve LIM2 wind and oceanic stress over ice, contrary to Roy et al. (2015). We noted some obvious differences between H02 and T321. For instance, the freshwater content of the Beaufort Sea in T321 does not reproduce the observed increase whereas H02 does. However, T321 has a more reasonable pattern of ice thickness and its March ice drift-velocity is the closest to observations. These differences could point to differences in atmospheric forcing, although we cannot exclude other model errors such as the noted overestimation of the air-ice stress in H02 (i.e., too strong Ekman transport and pumping) and possibly too strong vertical mixing in all configurations².

Finally, different advances in ice modelling and ice-ocean coupling are of interest to this project. First, although not critical for the type of evaluation done here, there is a strong incentive (Hibler, 2001; Campin et al., 2008; Griffies et al., 2011) in moving to a more exact “embedded” sea-ice representation in the ocean water column (ice loading effect, volume exchange, true salt flux, implicit momentum coupling between ice and ocean) with possible impacts in shallow channels where ice pressure ridges could restrain the passage of water underneath. This will be tested in the upcoming future. Second, a landfast ice parametrization (Lemieux et al., 2015b) should improve the representation of ice dynamics over the shelves, especially on the Siberian side, and we are hopeful for results in the very near future in this area as well. Third, two-way coupling between the wave field, the ocean and the ice are in progress (Dumont et al., 2011) and are expected to improve substantially the upper ocean response (with the addition of Stokes currents and induced mixing), the representation of the ice in the marginal ice zone, and improving the wave field in general.

Additionally, promising advances in the parametrization of form drag (Tsamados et al., 2014) between ice-air and sea-ice, and rheology (Tsamados et al., 2013) need to be implemented and tested, although for the latter, it is not clear how beneficial this new rheology can be at high resolution – which is true of any existing rheology for that matter. The two latter advances are already available in CICE5 (Turner and Hunke, 2014). We also plan to move to NEMO Version 3.6 in the upcoming future, which will offer support for coupling to CICE5. We are finally hopeful to increase the vertical resolution of the ocean component to 75 levels with a limit to 250 m thick layers in the deep ocean, instead of the present 450 m limit. This would put us on par with DRAKKAR and Mercator-Océan’s latest standards used in research.

²Note that the background diffusivity value used in our hindcasts is ten folds the one recommended by Zhang and Steele (2007)

Acknowledgements. This research was made possible thanks to fundings from METAREA and BREA. The Gewex data was obtained from the NASA Langley Research Center Atmospheric Science Data Center. The altimeter products were produced by Ssalto/Duacs and distributed by Aviso, with support from Cnes (<http://www.aviso.altimetry.fr/duacs/>). The reanalysis products (GLORYS) and the observational data CORA3.4 were accessed through MyOcean. The BGEP and ITP data was downloaded from Woods Hole Oceanographic Institute. We are grateful for NSIDC for providing ice concentration and velocity products, Sinead Farrell for the Arctic MDT and IABP for arctic buoy data. Finally, the manuscript benefited from the insightful comments of Daniel Deacu and two anonymous reviewers.

References

- Amante, C. and Eakins, B. W.: ETOPO1 1-Arc-Minute Global Relief Model: Procedures, Data Sources and Analysis, Tech. rep., NOAA Technical Memorandum NESDIS NGDC-24, National Geophysical Data Center, NOAA, doi:10.7289/V5C8276M, 2009.
- 665 Barnier, B., Madec, G., Penduff, T., Molines, J.-M., Tréguier, A.-M., Sommer, J. L., Beckmann, A., Bias-toch, A., Böning, C., Dengg, J., Derval, C., Durand, E., Gulev, S., Rémy, E., Talandier, C., Theetten, S., Maltrud, M. E., McClean, J., and Cuevas, B. D.: Impact of partial steps and momentum advection schemes in a global ocean circulation model at eddy permitting resolution, *Ocean Dyn.*, 56, 543–567, doi:10.1007/s10236-006-0082-1, 2006.
- 670 Bélair, S., Roch, M., Leduc, A.-M., Vaillancourt, P. A., Laroche, S., and Mailhot, J.: Medium-range quantitative precipitation forecasts from Canada’s new 33-km deterministic global operational system, *Weather and Forecasting*, 24, 690–708, doi:10.1175/2008WAF2222175.1, 2009.
- Benveniste, J.: Radar altimetry: past, present and future, in: *Coastal Altimetry*, edited by Vignudelli, S., Kostianoy, A., Cipolline, P., and Benveniste, J., chap. 1, pp. 1–17, Springer-Verlag, doi:10.1007/978-3-642-12796-0_1, 2011.
- 675 Blanke, B. and Delecluse, P.: Variability of the tropical Atlantic Ocean simulated by a general circulation model with two different mixed-layer physics, *J. Phys. Oceanogr.*, 23, 1363–1388, 1993.
- Blockley, E. W., Martin, M. J., McLaren, A. J., Ryan, A. G., Waters, J., Lea, D. J., Mirouze, I., Peterson, K. A., Sellar, A., , and Storkey, D.: Recent development of the Met Office operational ocean forecasting system: an overview and assessment of the new Global FOAM forecasts, *Geosci. Model Dev.*, 7, 2613–2638, doi:10.5194/gmd-7-2613-2014, 2014.
- 680 Bouillon, S., Morales Maqueda, M. A., Legat, V., and Fichet, T.: An elastic-viscous-plastic sea ice model formulated on Arakawa B and C grids, *Ocean Model.*, 27, 174–184, doi:10.1016/j.ocemod.2009.01.004, 2009.
- 685 Campin, J.-M., Marshall, J., and Ferreira, D.: Sea ice-ocean coupling using a rescaled vertical coordinate z^* , *Ocean Modelling*, 24, 1–14, doi:10.1016/j.ocemod.2008.05.005, 2008.
- Cavalieri, D. C., Parkinson, C., Gloersen, P., and Zwally, H. J.: Sea ice concentrations from NIMBUS-7 SMMR and DMSP SSM/I passive microwave data, [1979-2006], Tech. rep., National Snow and Ice Data Center, Boulder, Colorado USA, digital media, 1996, updated 2008.
- 690 Comiso, J. C., Cavalieri, D. J., Parkinson, C. L., and Gloersen, P.: Passive microwave algorithms for sea ice concentration: A comparison of two techniques, *Remote sensing of Environment*, 60, 357–384, 1997.
- Curry, B., Lee, C., Petrie, B., Moritz, R., and Kwok, R.: Multi-year volume, liquid freshwater, and sea ice transports through Davis Strait, 2004-2010, *J. Phys. Oceanogr.*, pp. 1244–1266, doi:10.1175/JPO-D-13-0177.1, 2013.
- 695 Dai, A. and Trenberth, K. E.: Estimates of freshwater discharge from continents: Latitudinal and seasonal variations, *Journal of hydrometeorology*, 3, 660–687, 2002.
- Drakkar Group: Eddy permitting ocean circulation hindcasts of past decades, *Clivar Exchanges*, 12, 8–10, 2007.
- Drillet, Y., Bourdallé-Badie, R., Siefridt, L., and Provost, C. L.: Meddies in the Mercator North Atlantic and Mediterranean Sea eddy-resolving model, *J. Geophys. Res.*, 110, C03 016, doi:10.1029/2003JC002170, 700 2005.

Dumont, D., Kohout, A., and Bertino, L.: A wave-based model for the marginal ice zone including a floe breaking parameterization, *J. Geophys. Res.*, 116, C04 001, doi:10.1029/2010JC006682, 2011.

Dupont, F., Hannah, C. G., and Wright, D. G.: Model investigation of the Slope Water, north of the Gulf Stream, *Geophys. Res. Lett.*, 33, L05 604, doi:10.1029/2005GL025321, 2006.

705 Dupont, F., Chittibabu, P., Fortin, V., Rao, Y. R., and Lu, Y.: Assessment of a NEMO-based hydrodynamic modelling system for the Great Lakes, *Water Quality Research Journal of Canada*, 47, 198–214, doi:10.2166/wqrjc.2012.014, 2012.

Fahrbach, E., Meincke, J., Østerhus, S., Rohardt, G., Schauer, U., Tverberg, V., and Verduin, J.: Direct measurements of volume transports through Fram Strait, *Polar Research*, 20, 217–224, 2001.

710 Farrell, S. L., McAdoo, D. C., Laxon, S. W., Zwally, H. J., Yi, D., Ridout, A., and Giles, K.: Mean dynamic topography of the Arctic Ocean, *Geophys. Res. Lett.*, 39, L01 601, doi:10.1029/2011GL050052, 2012.

Ferry, N., Parent, L., Garric, G., Bricaud, C., Testut, C.-E., Galloudec, O. L., Lellouche, J.-M., Drevillon, M., Greiner, E., Barnier, B., Molines, J.-M., Jourdain, N. C., Guinehut, S., Cabanes, C., and Zawadzki, L.: GLORYS2V1 global ocean reanalysis of the altimetric era (1992-2009) at meso scale, *Mercator Quarterly Newsletter*, 44, 29–39, available at <http://www.mercator-ocean.fr/eng/actualites-agenda/newsletter>, 2012.

715 Fichefet, T. and Maqueda, M. A. M.: Sensitivity of a global sea ice model to the treatment of ice thermodynamics and dynamics, *J. Geophys. Res.*, 102, 12 609–12 646, doi:10.1029/97JC00480, 1997.

Fowler, C., Emery, W., and Tschudi, M.: Polar Pathfinder Daily 25 km EASE-Grid Sea Ice Motion Vectors. Version 2 [2002-2009], Tech. rep., Boulder, Colorado USA: NASA DAAC at the National Snow and Ice Data Center., 2013.

720 Gaspar, P., Gregoris, Y., and Lefevre, J. M.: A simple eddy kinetic energy model for simulations of the oceanic vertical mixing: Tests at station Papa and long-term upper ocean study site, *J. Geophys. Res.*, 95, 16 179–16 193, 1990.

Griffies, S. M., Winton, M., Donner, L. J., Horowitz, L. W., Downes, S. M., Farneti, R., Gnanadesikan, A., 725 Hurlin, W. J., Lee, H.-C., Liang, Z., Palter, J. B., Samuels, B. L., Wittenberg, A. T., Wyman, B. L., Yin, J., and Zadeh, N.: The GFDL CM3 Coupled Climate Model: Characteristics of the Ocean and Sea Ice Simulations, *J. Climate*, 24, 13 520–13 544, doi:10.1175/2011JCLI3964.1, 2011.

Hamilton, J. M., Collins, K., and Prinsenberg, S. J.: Links between ocean properties, ice cover, and plankton dynamics on interannual time scales in the Canadian Arctic Archipelago, *J. Geophys. Res.*, 118, 5625–5639, 730 doi:10.1002/jgrc.20382, 2013.

Hewitt, H. T., Copsey, D., Culverwell, I. D., Harris, C. M., Hill, R. S. R., Keen, A. B., McLaren, A. J., and Hunke, E. C.: Design and implementation of the infrastructure of HadGEM3: the next-generation Met Office climate modelling system, *Geosci. Model Dev.*, 4, 223–253, doi:10.5194/gmd-4-223-2011, 2011.

Hibler, W.: Modeling the formation and evolution of oriented fractures in sea ice, *Annals of Glaciology*, 33, 735 157–164, 2001.

Hibler, III, W. D.: A dynamic thermodynamic sea ice model, *J. Phys. Oceanogr.*, 9, 815–843, 1979.

Higginson, S., Thompson, K. R., Huang, J., Véronneau, M., and Wright, D. G.: The mean surface circulation of the North Atlantic subpolar gyre: A comparison of estimates derived from new gravity and oceanographic measurements, *J. Geophys. Res.*, 116, C08 016, doi:10.1029/2010JC006877, 2011.

- 740 Holloway, G. and Wang, Z.: Representing eddy stress in an Arctic Ocean model, *J. Geophys. Res.*, 114, C06 020, doi:10.1029/2008JC005169, 2009.
- Hunke, E. C.: Viscous-plastic sea ice dynamics with the EVP model: linearization issues, *J. Comput. Physics*, 170, 18–38, 2001.
- Hunke, E. C. and Dukowicz, J. K.: An elastic-viscous-plastic model for sea ice dynamics, *J. Phys. Oceanogr.*, 27, 1849–1867, 1997.
- 745 Hunke, E. C. and Dukowicz, J. K.: The Elastic-Viscous-Plastic Sea Ice Dynamics Model in General Orthogonal Curvilinear Coordinates on a Sphere–Incorporation of Metric Terms, *Monthly Weather Review*, 130, 1848–1865, 2002.
- Hunke, E. C. and Lipscomb, W. H.: CICE: the Los Alamos Sea Ice Model Documentation and Software User’s Manual, Tech. rep., Los Alamos National Laboratory, 2010.
- 750 Jakobson, E., Vihma, T., Palo, T., Jakobson, L., Keernik, H., and Jaagus, J.: Validation of atmospheric reanalyses over the central Arctic Ocean, *Geophys. Res. Lett.*, 39, L10 802, doi:10.1029/2012GL051591, 2012.
- Kwok, R. and Morison, J.: Dynamic topography of the ice-covered Arctic Ocean from ICESat, *Geophysical Research Letters*, 38, L02 501, doi:10.1029/2010GL046063, 2011.
- 755 Kwok, R., Cunningham, G., and Pang, S.: Fram Strait sea ice outflow, *Journal of Geophysical Research: Oceans* (1978–2012), 109, doi:10.1029/2003JC001785, 2004.
- Kwok, R., Cunningham, G. F., Wensnahan, M., Rigor, I., Zwally, H. J., and Yi, D.: Thinning and volume loss of Arctic sea ice cover: 2003–2008, *J. Geophys. Res.*, 114, C07 005, doi:10.1029/2009JC005312, 2009.
- Laxon, S., Giles, K. A., Ridout, A. L., Wingham, D. J., Willatt, R., Cullen, R., Kwok, R., Schweiger, A., Zhang, J., Haas, C., Hendricks, S., Krishfield, R., Kurtz, N., Farrell, S., and Davidson, M.: CryoSat-2 estimates of Arctic sea ice thickness and volume, *Geophys. Res. Lett.*, 40, 1–6, doi:10.1002/GRL.50193, 2013.
- 760 Lemieux, J.-F., Beaudoin, C., Dupont, F., Roy, F., Smith, G. C., Shlyaeva, A., Buehner, M., Caya, A., Chen, J., Carrieres, T., Pogson, L., DeRepentigny, P., Plante, A., Pestieau, P., Pellerin, P., Ritchie, H., Garric, G., and Ferry, N.: The Regional Ice Prediction System (RIPS): verification of forecast sea ice concentration, *Q. J. R. Meteorol. Soc.*, p. in press, doi:10.1002/qj.2526, 2015a.
- 765 Lemieux, J.-F., Tremblay, B., Dupont, F., Plante, M., Smith, G., and Dumont, D.: A basal stress parameterization for modeling landfast ice, *J. Geophys. Res.*, 2015b.
- Lipscomb, W. H., Hunke, E. C., Maslowski, W., and Jakacki, J.: Ridging, strength, and stability in high-resolution sea ice models, *J. Geophys. Res.*, 112, C03S91, doi:10.1029/2005JC003355, 2007.
- 770 Lique, C., Garric, G., Treguier, A.-M., Barnier, B., Ferry, N., Testut, C.-E., and Girard-Ardhuin, F.: Evolution of the Arctic Ocean Salinity, 2007–2008: Contrast between the Canadian and the Eurasian Basins, *J. Climate*, 24, 1705–1717, doi:10.1175/2010JCLI3762.1, 2011.
- Lu, Y., Higginson, S., Nudds, S., and Prinsenber, S.: Model simulated volume fluxes through the Canadian Arctic Archipelago and Davis Strait: Linking monthly variations to forcing in different seasons, *Journal of Geophysical Research: Oceans*, 119, 1927–1942, doi:10.1002/2013JC009408, 2014.
- 775 Lumpkin, R. and Johnson, G. C.: Global ocean surface velocities from drifters: Mean, variance, El Niño–Southern Oscillation response, and seasonal cycle, *J. Geophys. Res.*, 118, 1–15, doi:10.1002/jgrc.20210, 2013.

- Madec, G. and NEMO team: NEMO ocean engine, Tech. rep., Note du Pole de Modelisation, 27, Institut Pierre-Simon Laplace, 11, 2008.
- Madec, G., Delecluse, P., Imbard, M., and Lévy, C.: OPA 8.1. Ocean General Circulation Model reference manual, Tech. rep., Note du Pole de Modelisation, Institut Pierre-Simon Laplace, 11, 1998.
- Masson-Delmotte, V., Kageyama, M., Braconnot, P., Charbit, S., Krinner, G., Ritz, C., Guilyardi, E., Jouzel, J., Abe-Ouchi, A., Crucifix, M., Gladstone, R. M., Hewitt, C. D., Kitoh, A., LeGrande, A. N., Marti, O., Merkel, U., Motoi, T., Ohgaito, R., Otto-Bliesner, B., Peltier, W. R., Ross, I., Valdes, P. J., Vettoretti, G., Weber, S. L., Wolk, F., and Yu, Y.: Past and future polar amplification of climate change: climate model intercomparisons and ice-core constraints, *Climate Dynamics*, 26, 513–529, doi:10.1007/s00382-005-0081-9, 2006.
- Massonnet, F., Fichefet, T., Goosse, H., Vancoppenolle, M., Mathiot, P., and König Beatty, C.: On the influence of model physics on simulations of Arctic and Antarctic sea ice, *The Cryosphere*, 5, 687–699, doi:10.5194/tc-5-687-2011, 2011.
- Maykut, G. A. and McPhee, M. G.: Solar heating of the Arctic mixed layer, *J. Geophys. Res.*, 100, 24 691–24 703, 1995.
- McPhee, M. G.: Ice-ocean momentum transfer for the AIDJEX ice model, *AIDJEX Bulletin*, 29, 93–111, 1975.
- Megann, A., Storkey, D., abd S. Alderson, Y. A., Calvert, D., Graham, T., Hyder, P., Siddorn, J., and Sinha, B.: GO5.0: The joint NERC-Met Office NEMO global ocean model for use in coupled and forced applications, *GeoSci. Model Dev. Discuss.*, 6, 5747–5799, 2014.
- Morison, J., Aagaard, K., Falkner, K. K., Hatakeyama, K., Moritz, R., Overland, J. E., Perovich, D., Shimada, K., Steele, M., Takizawa, T., and Woodgate, R.: North Pole Environmental Observatory delivers early results, *Eos, Transactions American Geophysical Union*, 83, 357–361, doi:10.1029/2002EO000259, 2002.
- Pickart, R. S., McKee, T. K., Torres, D. J., and Harrington, S.: Mean Structure and Interannual Variability of the Slope Water System South of Newfoundland, *J. Phys. Oceanogr.*, 29, 2541–2558, 1999.
- Polashenski, C., Perovich, D., Richter-Menge, J., and Elder, B.: Seasonal ice mass-balance buoys: adapting tools to the changing Arctic, *Annals of Glaciology*, 52, 18–26, 2011.
- Proshutinsky, A., Krishfield, R., Timmermans, M.-L., Toole, J., Carmack, E., McLaughlin, F., Williams, W. J., Zimmermann, S., Itoh, M., and Shimada, K.: Beaufort Gyre freshwater reservoir: State and variability from observations, *J. Geophys. Res.*, 114, C00A10, doi:10.1029/2008JC005104, 2009.
- Rattan, S., Myers, P. G., Treguier, A.-M., Theetten, S., Biastoch, A., and Böning, C.: Towards an understanding of Labrador Sea salinity drift in eddy-permitting simulations, *Ocean Modelling*, 35, 77–88, doi:10.1016/j.ocemod.2010.06.007, 2010.
- Rio, M. H., Guinehut, S., and Larnicol, G.: New CNES-CLS09 global mean dynamic topography computed from the combination of GRACE data, altimetry, and in situ measurements, *J. Geophys. Res.*, 116, C07 018, doi:10.1029/2010JC006505, 2011.
- Rothrock, D. A.: The Energetics of the Plastic Deformation of Pack Ice by Ridging, *J. Geophys. Res.*, 33, 4514–4519, 1975.
- Roy, F., Chevallier, M., Smith, G., Dupont, F., Garric, G., and Lemieux, J.-F.: Arctic sensitivity to the atmosphere-ice-ocean boundary layer in global simulations, *J. Geophys. Res.*, in revision, 2015.

- Saenko, O. A., Dupont, F., Yang, D., Myers, P. G., Yashayaev, I., and Smith, G. C.: Role of Resolved and Parameterized Eddies in the Labrador Sea Balance of Heat and Buoyancy, *J. Phys. Oceanogr.*, 44, doi:10.1175/JPO-D-14-0041.1, 2014.
- 820 Schauer, U., Fahrbach, E., Osterhus, S., and Rohardt, G.: Arctic warming through the Fram Strait: Oceanic heat transport from 3 years of measurements, *J. Geophys. Res.*, 109, C06 026, doi:10.1029/2003JC001823, 2004.
- Schauer, U., Beszczynska-Möller, A., Walczowski, W., Fahrbach, E., Piechura, J., and Hansen, E.: Variation of Measured Heat Flow Through the Fram Strait Between 1997 and 2006, in: *Arctic-Subarctic Ocean Fluxes*, edited by Dickson, R., Meincke, J., and Rhines, P., pp. 65–85, Springer Netherlands, doi:10.1007/978-1-4020-6774-7_4, 2008.
- 825 Smith, G. C., Roy, F., and Brasnett, B.: Evaluation of an operational ice-ocean analysis and forecasting system for the Gulf of St Lawrence, *Q. J. R. Meteorol. Soc.*, 139, 419–433, doi:10.1002/qj.1982, 2012.
- Smith, G. C., Roy, F., Mann, P., Dupont, F., Brasnett, B., Lemieux, J.-F., Laroche, S., and Belair, S.: A new atmospheric dataset for forcing ice-ocean models: Evaluation of reforecasts using the Canadian global deterministic prediction system, *Q. J. R. Meteorol. Soc.*, 140, 881–894, doi:10.1002/qj.2194, 2014.
- 830 Smith, G. C., Roy, F., Reszka, M., Colan, D. S., He, Z., Deacu, D., Belanger, J.-M., Skachko, S., Liu, Y., Dupont, F., Jean-Fran c. L., Beaudoin, C., Tranchant, B., Drevillon, M., Garric, G., Testut, C.-E., Lellouche, J.-M., Pellerin, P., Ritchie, H., Lu, Y., and Davidson, F.: Sea ice Forecast Verification in the Canadian Global Ice Ocean Prediction System, *Q. J. R. Meteorol. Soc.*, doi:10.1002/qj2555, accepted, 2015.
- 835 Steele, M.: Sea ice melting and floe geometry in a simple ice-ocean model, *J. Geophys. Res.*, 97, 17 729–17 738, 1992.
- Steele, M., Morison, J., Ermold, W., Rigor, I., Ortmeyer, M., and Shimada, K.: Circulation of summer Pacific halocline water in the Arctic Ocean, *J. Geophys. Res.*, 109, C02 027, doi:10.1029/2003JC002009, 2004.
- Talley, L., Pickard, G., Emery, W., and Swift, J.: *Descriptive physical oceanography: an introduction*, 6th edn., Academic Press, London, 2011.
- 840 Thompson, K. and Demirov, E.: Skewness of sea level variability of the world’s oceans, *J. Geophys. Res.*, 111, C05 005, doi:10.1029/2004JC002839, 2006.
- Tsamados, M., Feltham, D. L., and Wilchinsky, A. V.: Impact of a new anisotropic rheology on simulations of Arctic sea ice, *J. Geophys. Res.*, 118, 91–107, doi:10.1029/2012JC007990, 2013.
- 845 Tsamados, M., Feltham, D. L., Schroeder, D., Flocco, D., Farrell, S. L., Kurtz, N., Laxon, S. W., and Bacon, S.: Impact of Variable Atmospheric and Oceanic Form Drag on Simulations of Arctic Sea Ice, *J. Phys. Oceanogr.*, 44, 1329–1353, doi:10.1175/JPO-D-13-0215.1, 2014.
- Turner, A. K. and Hunke, E. C.: Impacts of a mushy-layer thermodynamic approach in global sea-ice simulations using the CICE sea-ice model, *J. Geophys. Res.*, submitted, 2014.
- 850 Umlauf, L. and Burchard, H.: A generic length-scale equation for geophysical turbulence models, *J. Mar. Res.*, 61, 235–265, 2003.
- Vancoppenolle, M., Fichefet, T., and Goosse, H.: Simulating the mass balance and salinity of Arctic and Antarctic sea ice. 2. Importance of sea ice salinity variations, *Ocean Modelling*, 27, 54–69, 2009a.
- Vancoppenolle, M., Fichefet, T., Goosse, H., Bouillon, S., Madec, G., and Morales Maqueda, M.: Simulating the mass balance and salinity of Arctic and Antarctic sea ice. 1. Model description and validation, *Ocean Modelling*, 27, 33–53, doi:10.1016/j.ocemod.2008.10.005, 2009b.
- 855

Vertenstein, M., Craig, T., Henderson, T., Murphy, S., Jr, G. R. C., and Norton, N.: CCSM3.0 User's Guide, UCAR, www.cesm.ucar.edu/ccsm3.0, 2004.

Wang, Z., Lu, Y., Wright, D., and Dupont, F.: Sea ice sensitivity to the parameterisation of open water area, *J. of Oper. Ocean.*, 3, 3–9, 2010.

Zhang, J. and Rothrock, D. A.: Modeling global sea ice with a thickness and enthalpy distribution model in generalized curvilinear coordinates, *Monthly Weather Review*, 131, 845–861, 2003.

Zhang, J. and Steele, M.: Effect of vertical mixing on the Atlantic Water layer circulation in the Arctic Ocean, *Journal of Geophysical Research: Oceans* (1978–2012), 112, doi:10.1029/2006JC003732, 2007.

Zhu, J., Demirov, E., Dupont, F., and Wright, D.: Eddy-permitting simulations of the sub-polar North Atlantic: impact of the model bias on water mass properties and circulation, *Ocean Dynamics*, 60, 1177–1192, 2009.

List of Tables

- 1 Summary description of the different hindcasts produced to date. Dates are given in YYYYMMDD format. 29

List of Figures

870	1	CREG12 domain and horizontal resolution (in km). The 3000 m contour of the modelled bathymetry is overlaid. 30
	2	First Rossby radius of deformation (left, in km) and Rossby radius relative to the local resolution in log 2 (right). Grossly speaking, the r
	3	The mean (top), standard deviation (middle) and skewness (bottom) of sea surface height (in m) in the North Atlantic from satellite altim
	4	(Left) The estimated Arctic mean dynamic topography for the period 2003–2009, as described by Farrell et al. (2012). (Right) Modelled
	5	Mean current speed at 15 m depth, (top) from a drifter climatology, and (bottom) from hindcast H05 averaged for the period 2003–2009.
875	6	The mean model bias for temperature (left) and salinity (right), calculated as the model hindcast H05 estimate minus the observed value,
	7	Average temperature and salinity profiles within the boxes shown in the top panel. All available observations within each box during the
	8	Mean liquid freshwater content (in m) from the PHC climatology (left) and from hindcast H05 (right) for the period 2003–2009. The wh
	9	Time series of the estimated liquid freshwater content, averaged over the Beaufort Gyre, from Proshutinsky et al. (2009) and updates (bla
	10	The mean observed (top), modelled (hindcast H05, middle) and difference (modelled minus observed, bottom) temperature (left), salinity
880	11	As for Figure 10, but for Davis Strait. 40
	12	Monthly time series of total ice extent in the Arctic obtained from satellite observations (black, described as SMMR+SSM/I), the ORCA
	13	Ice concentration for September 2007 from NSIDC, the ORCA12 T321 run from Mercator Océan and CREG12 hindcasts H02 and H05.
	14	Difference (in m, model minus observation) between the sea ice thickness from hindcast H02 (left) and hindcast H05 (right) and measure
	15	Average ice thickness distributions from ULS measurements (blue) and hindcast H05 (green) at the Beaufort Gyre Exploration Project m
885	16	The mean ice thickness (in m) for October–November 2007 from ICESat, and the difference between ORCA12 T321 and CREG12 hinde
	17	Monthly time series of total ice volume in the Arctic obtained from PIOMAS (black), the ORCA12 T321 run from Mercator Océan (blue
	18	Average ice velocity (in ms^{-1}) for March 2003–2008 from NSIDC, the ORCA12 T321 run from Mercator Océan, and CREG12 hindcast
	19	Monthly timeseries of average bias in monthly ice speed (in ms^{-1}) relative to IABP buoys for NSIDC (black dashed), the ORCA12 T32

experiment name	initial & boundary conditions	lateral dyn. BC	ice model	turbulence scheme	notes
ORCA12-T321	Levitus	free-slip	LIM2	TKE	Started in 19990101. Air-ice drag of 1.5×10^{-3} ; ice-ocean drag of 1.0×10^{-2}
H01	GLORYS2v1	no-slip	LIM2	TKE	Started in 20020101. Air-ice drag of 1.63×10^{-3} ; same ice-ocean drag
H02	ORCA12-T321	free-slip	LIM2	TKE	Started in 20030101
H03	ORCA12-T321	free-slip	CICE	$k - \epsilon$	Started in 20030101, reduced Bering flow to mean 0.8 Sv. Top ice roughness of 5.0×10^{-4} m; icea-ocean drag of 5.36×10^{-3} .
H04	ORCA12-T321	free-slip	CICE	$k - \epsilon$	Increased ice-ocean drag relative to H03 to 2.32×10^{-2} corresponding to a bottom ice roughness of 3.0×10^{-2} m
H05	ORCA12-T321	free-slip	CICE	$k - \epsilon$	H04 with ice surface roughness as in CGRF (1.0×10^{-4} m)

Table 1. Summary description of the different hindcasts produced to date. Dates are given in YYYYMMDD format.

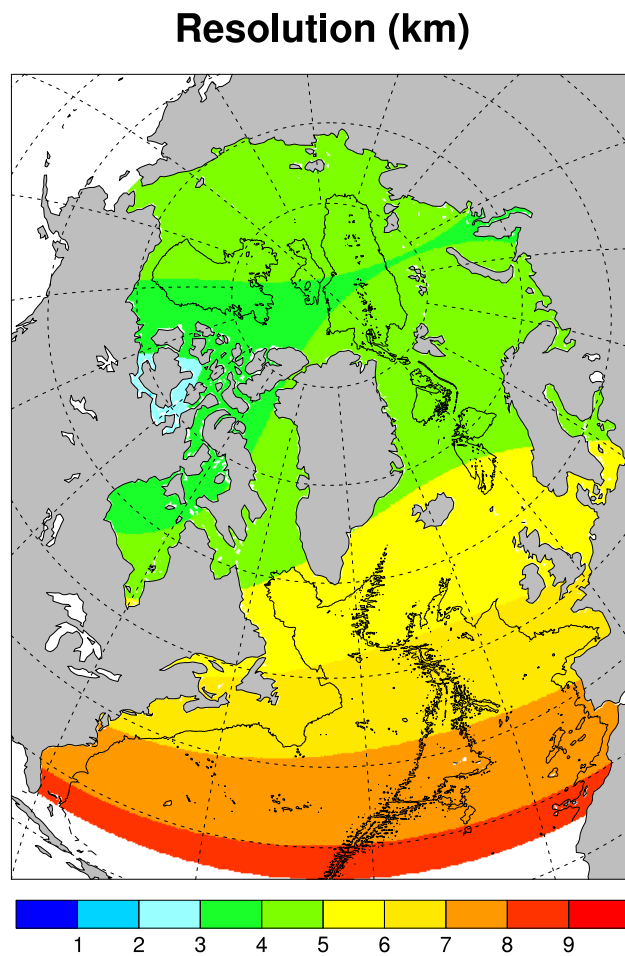


Figure 1. CREG12 domain and horizontal resolution (in km). The 3000 m contour of the modelled bathymetry is overlaid.

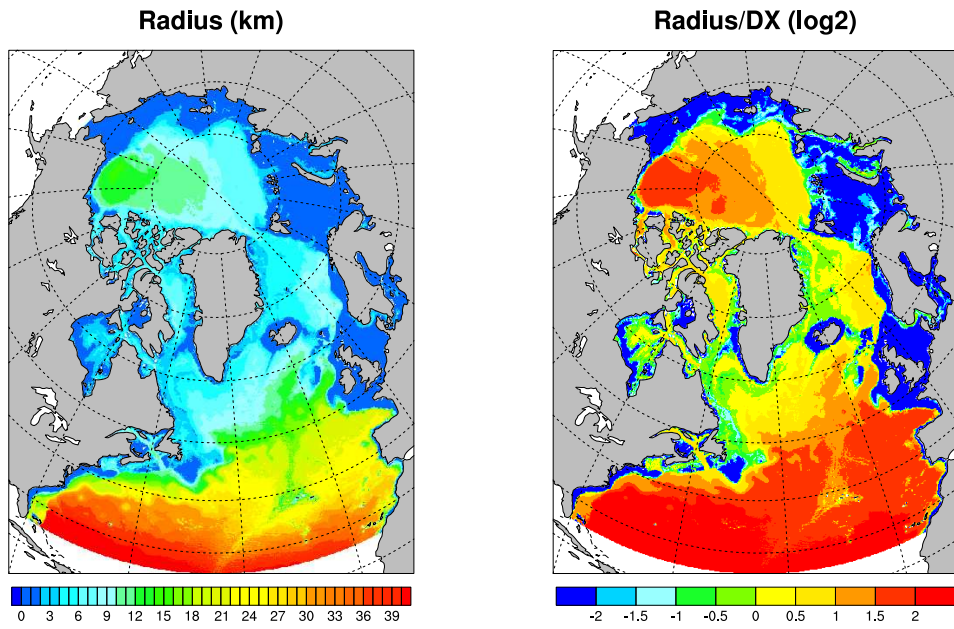


Figure 2. First Rossby radius of deformation (left, in km) and Rossby radius relative to the local resolution in log 2 (right). Grossly speaking, the right panel shows where model is eddy-resolving (values above 1, that is 2 model points to resolve a baroclinic eddy), eddy-permitting (between 0 and 1), or does not resolved eddies (values below 0.)

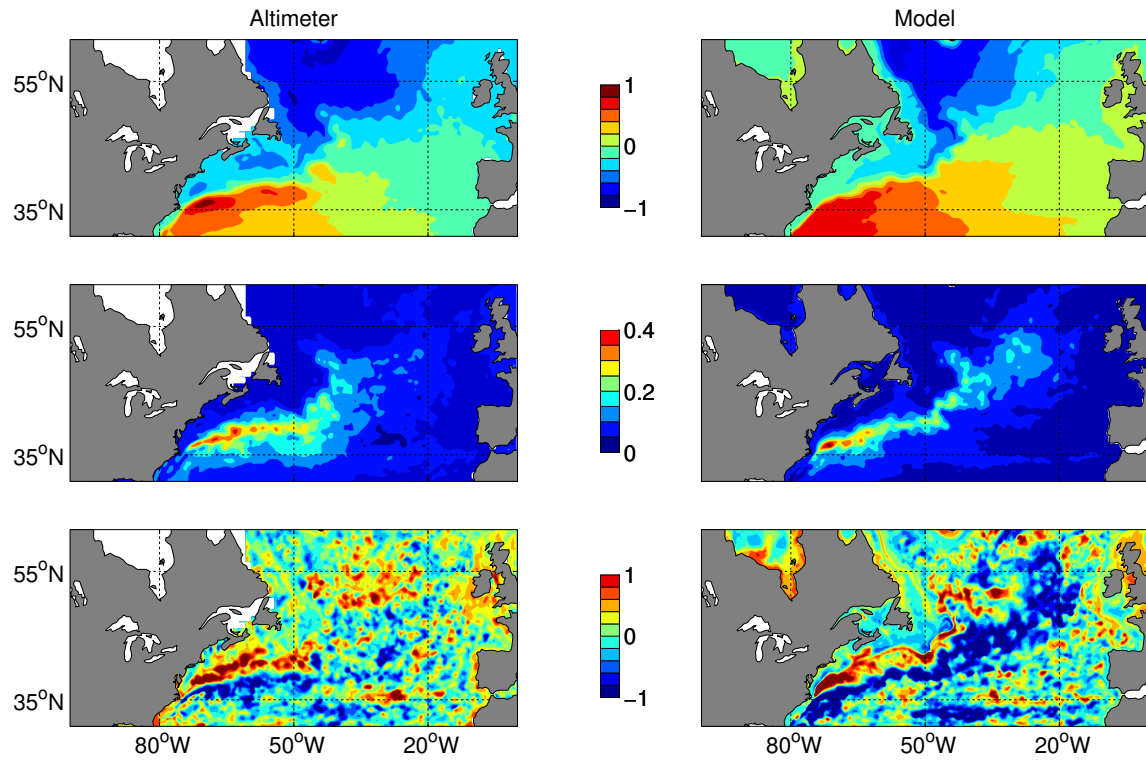


Figure 3. The mean (top), standard deviation (middle) and skewness (bottom) of sea surface height (in m) in the North Atlantic from satellite altimeter measurements (left) and the model hindcast H05 (right) for the period 2003–2009.

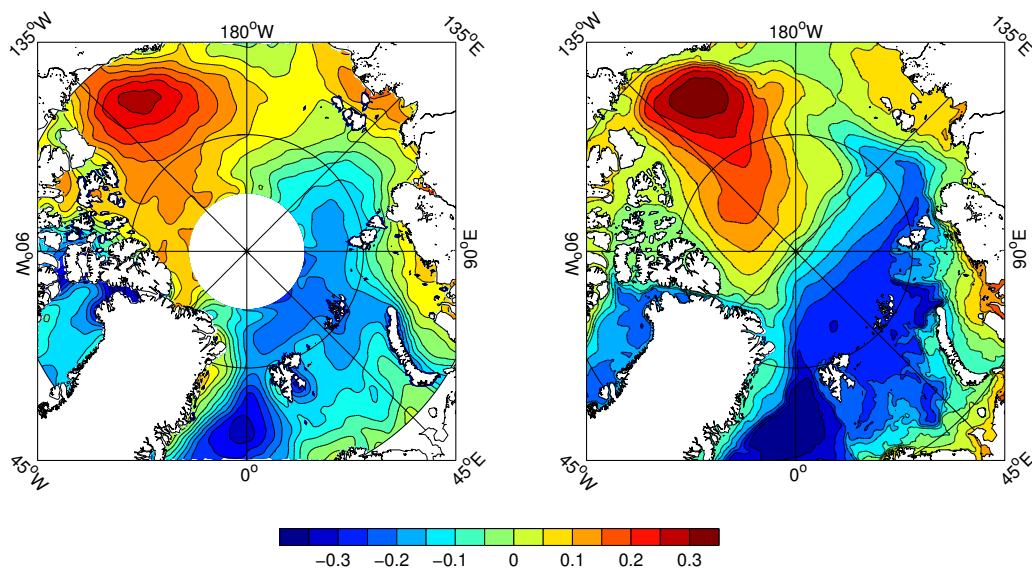


Figure 4. (Left) The estimated Arctic mean dynamic topography for the period 2003–2009, as described by Farrell et al. (2012). (Right) Modelled sea surface height (in m) in the Arctic for the period 2003–2009 from hindcast H05.

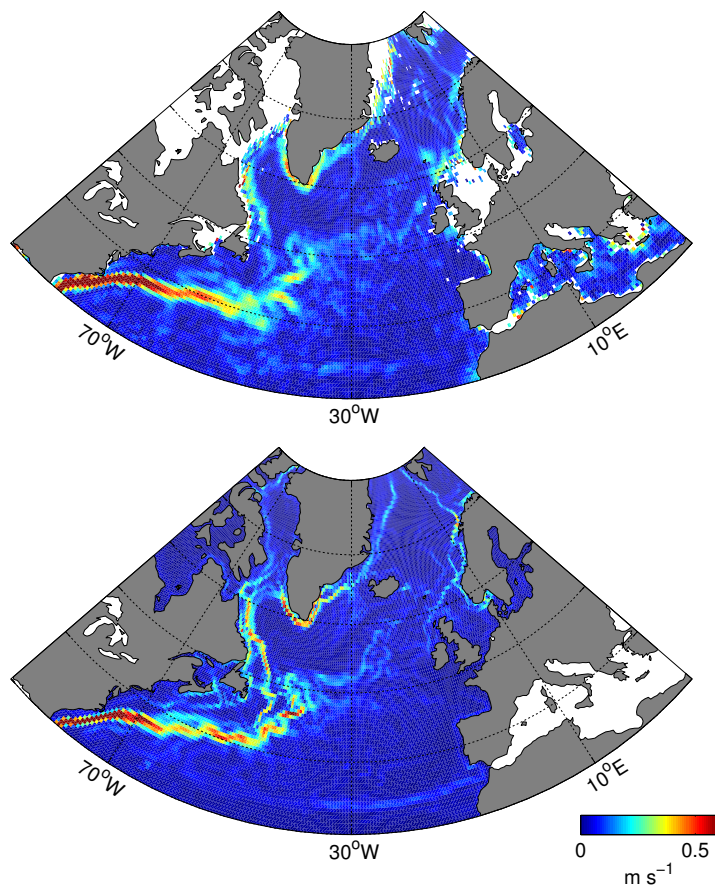


Figure 5. Mean current speed at 15 m depth, (top) from a drifter climatology, and (bottom) from hindcast H05 averaged for the period 2003–2009. The model output has been regridded to the same $1/2^\circ$ resolution as the drifter climatology.

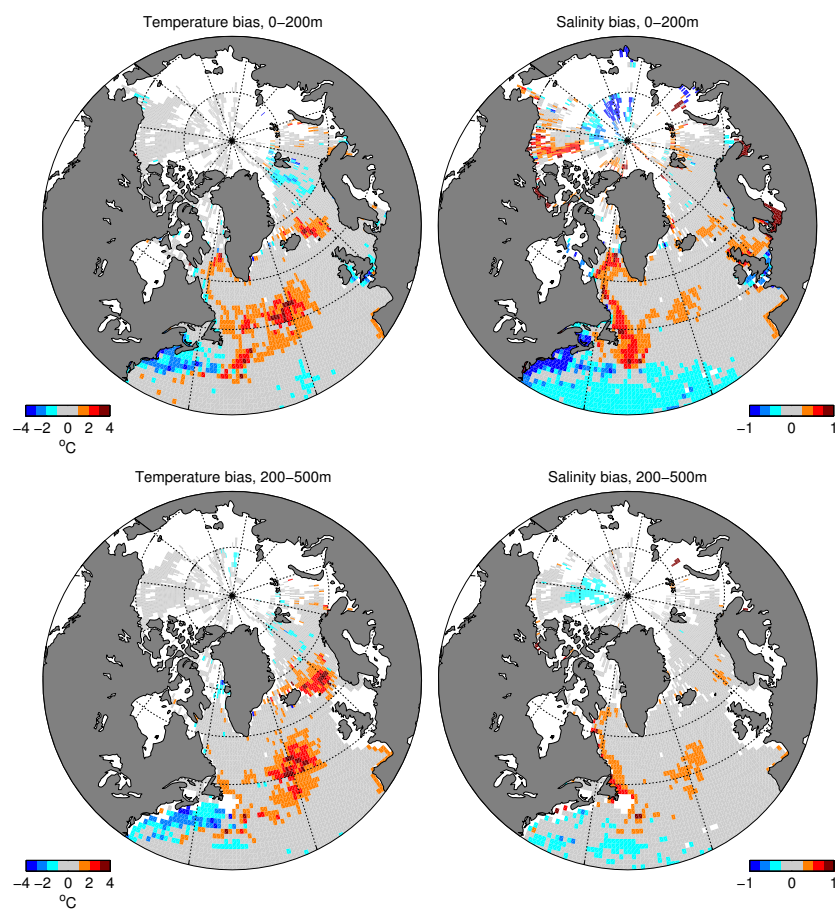


Figure 6. The mean model bias for temperature (left) and salinity (right), calculated as the model hindcast H05 estimate minus the observed value, averaged in 1 degree bins for the top 200 m (top) and the 200-500 m layer (bottom) for the period 2003–2009.

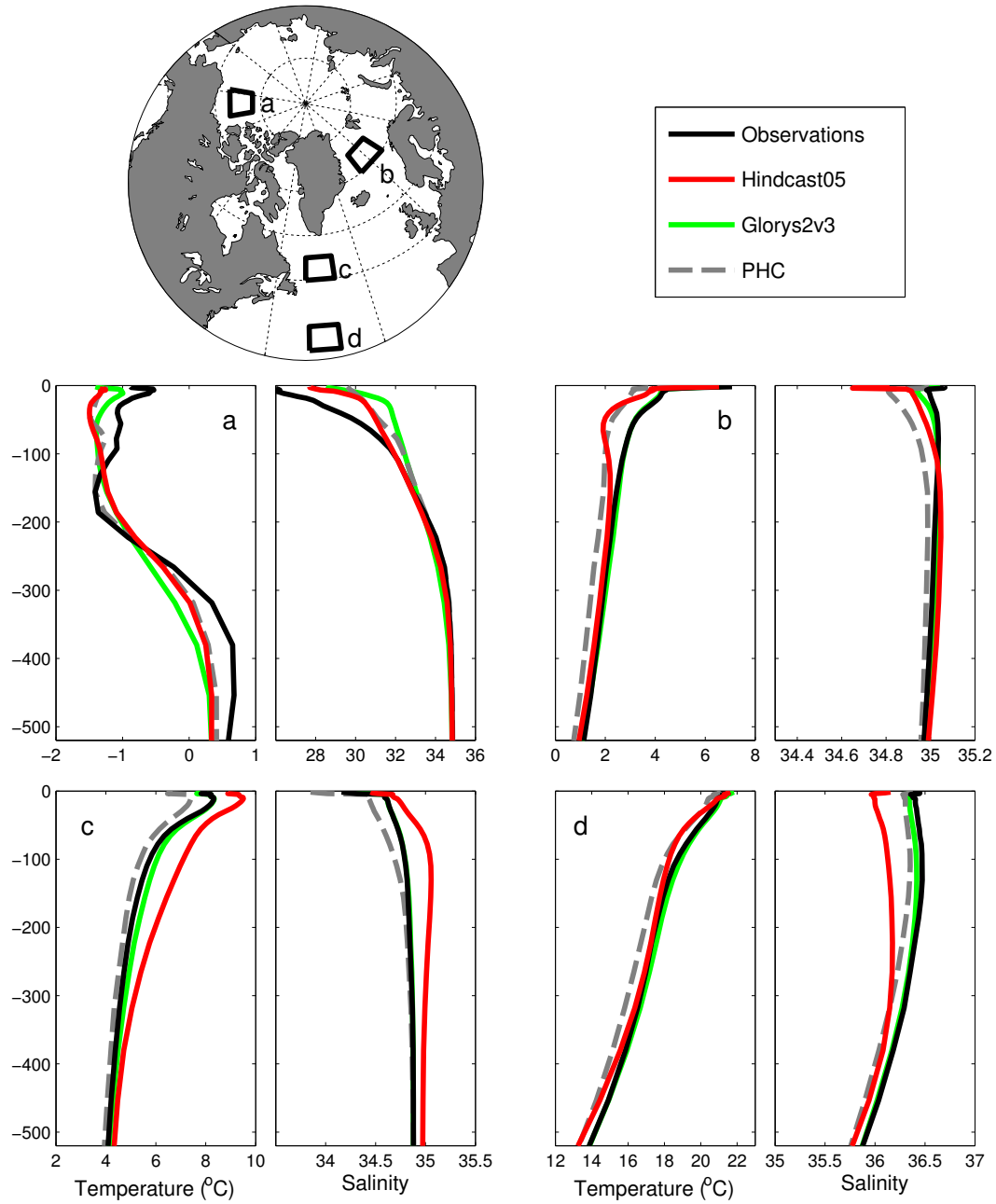


Figure 7. Average temperature and salinity profiles within the boxes shown in the top panel. All available observations within each box during the period 2003–2009 are averaged and plotted. Corresponding profiles from hindcast H05, the GLORYS2v3 ocean reanalysis, and the Polar Science Center Hydrographic Climatology (PHC), calculated in each case by averaging profiles at the same times and locations as the observations, are also shown. The boxes represent (a) the Beaufort Sea, 73° – 78° N, 152 – 132° W, (b) the Greenland and Norwegian seas, 70° – 75° N, 10° W– 10° E, (c) the subpolar gyre, 50° – 55° N, 50° – 40° W, and (d) the subtropical gyre, 35° – 40° N, 49° – 41° W. Note the different scaling on the horizontal axis for each panel.

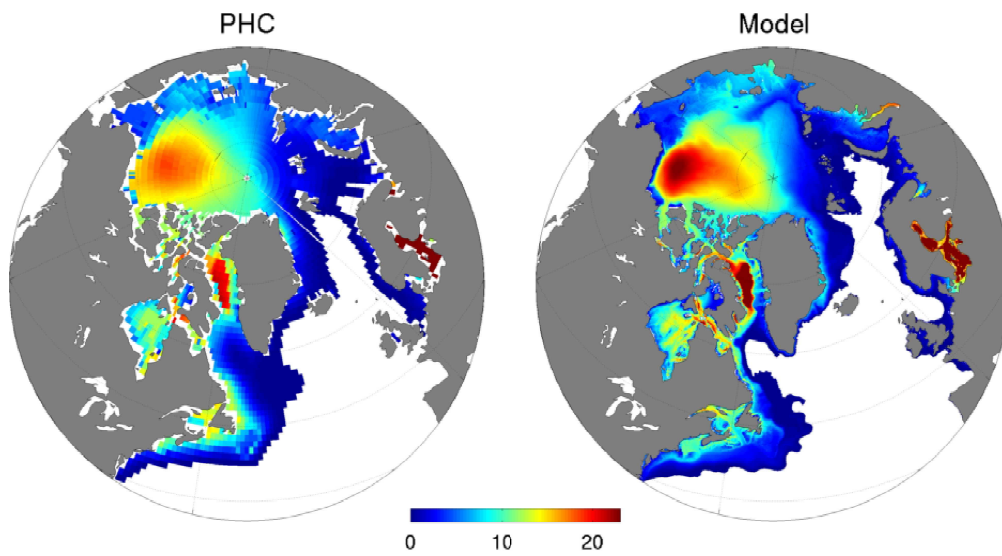


Figure 8. Mean liquid freshwater content (in m) from the PHC climatology (left) and from hindcast H05 (right) for the period 2003–2009. The white regions of the ocean correspond to regions where salinity at any depth is above the 34.8 reference salinity used to compute the freshwater content.

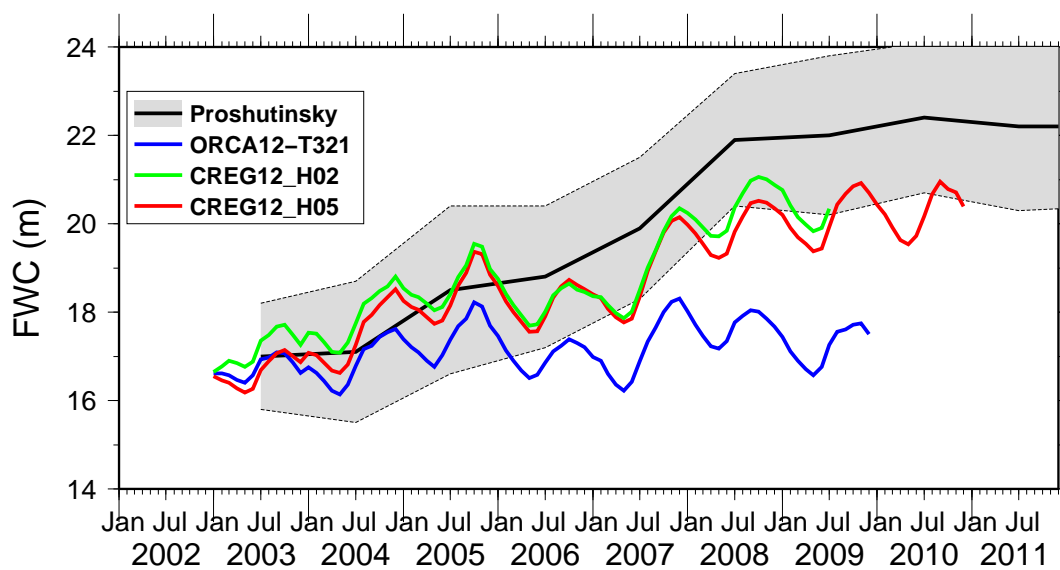


Figure 9. Time series of the estimated liquid freshwater content, averaged over the Beaufort Gyre, from Proshutinsky et al. (2009) and updates (black with uncertainties overlaid as grey area and bounded by dashed lines) compared with estimates from the ORCA12-T321 run from Mercator Océan (blue), and CREG12 hindcasts H02 (green) and H05 (red).

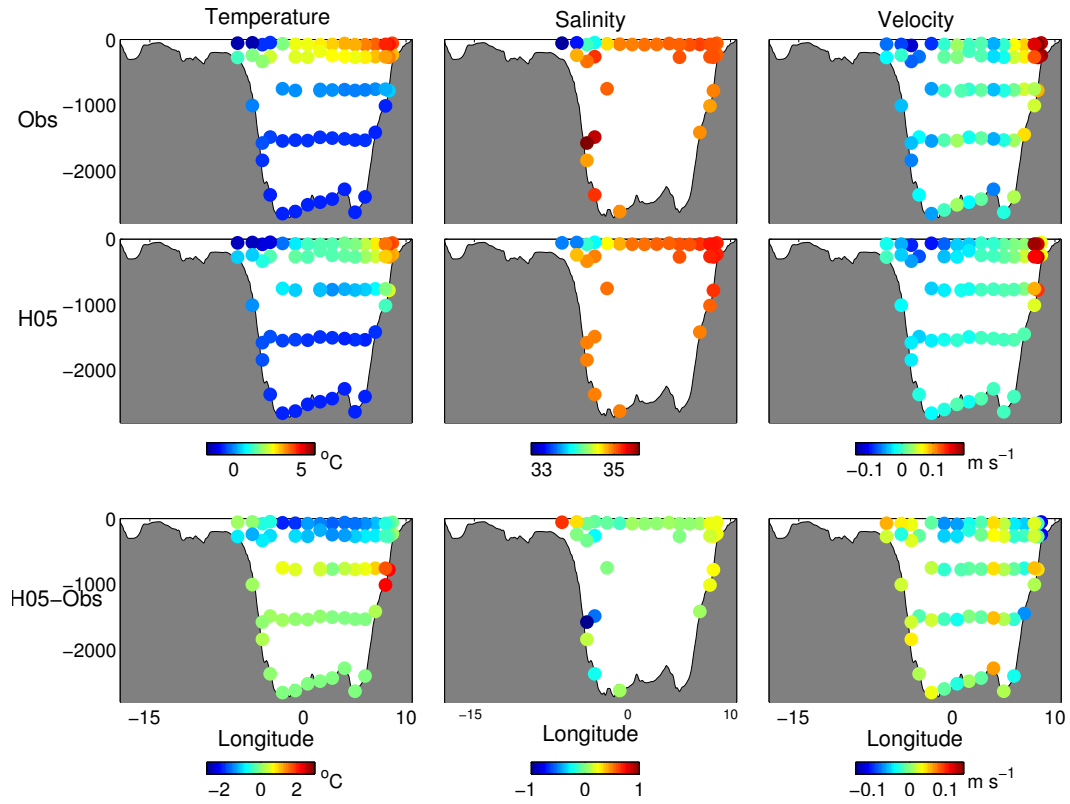


Figure 10. The mean observed (top), modelled (hindcast H05, middle) and difference (modelled minus observed, bottom) temperature (left), salinity (middle) and northward velocity (right) in Fram Strait.

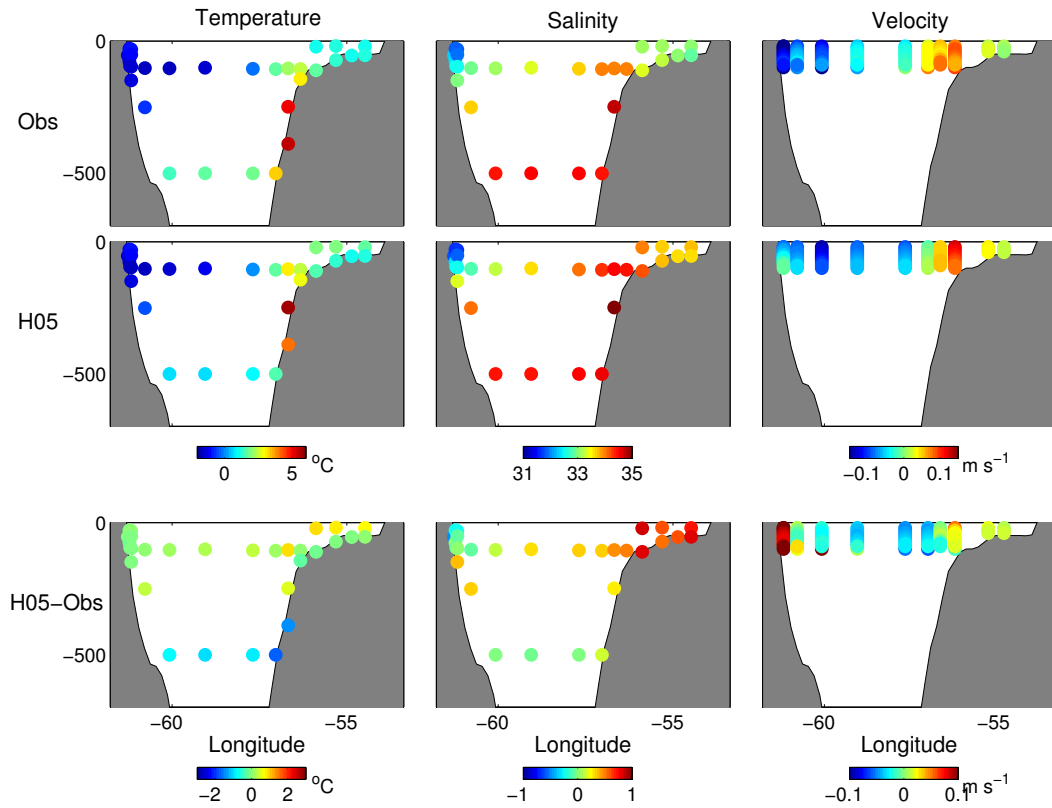


Figure 11. As for Figure 10, but for Davis Strait.

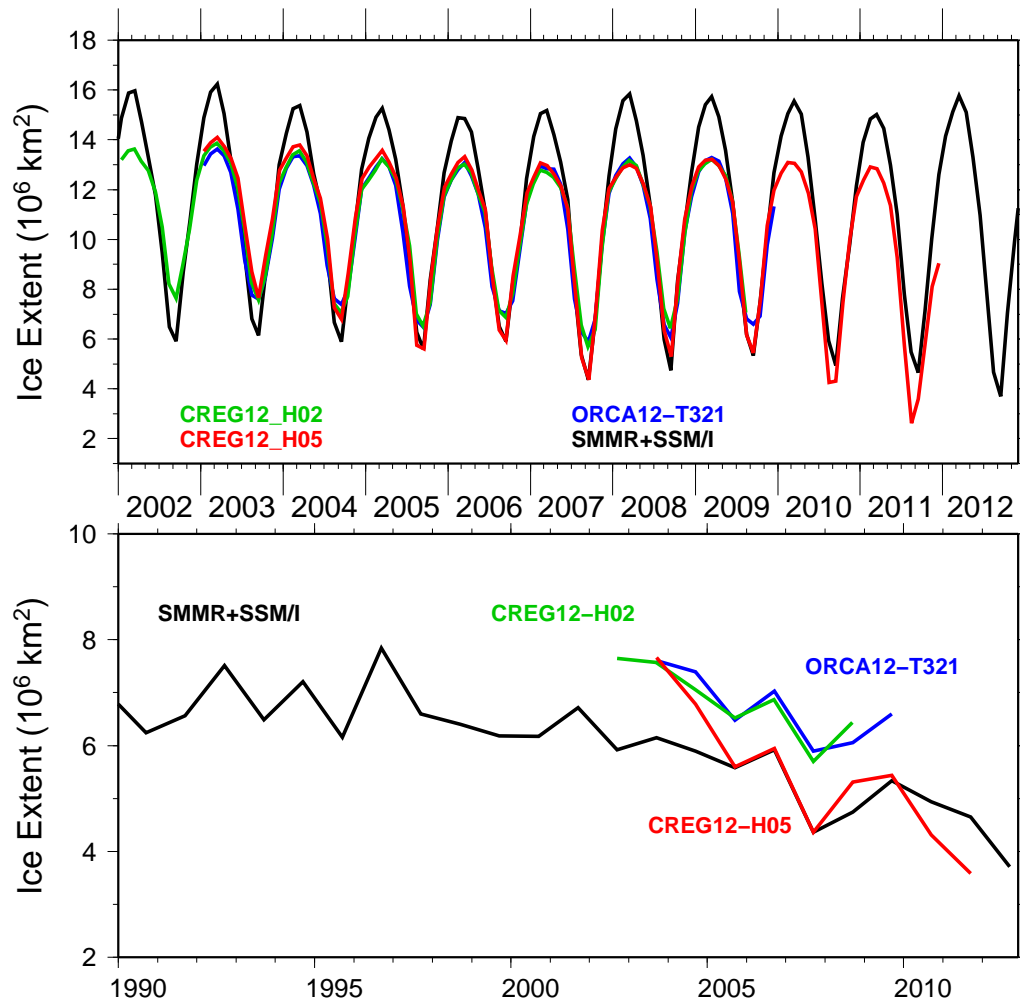


Figure 12. Monthly time series of total ice extent in the Arctic obtained from satellite observations (black, described as SMMR+SSM/I), the ORCA12 T321 run from Mercator Océan (blue), and CREG12 hindcasts H02 (green) and H05 (red). The top panel shows all months, the bottom panel retains only September from each year.

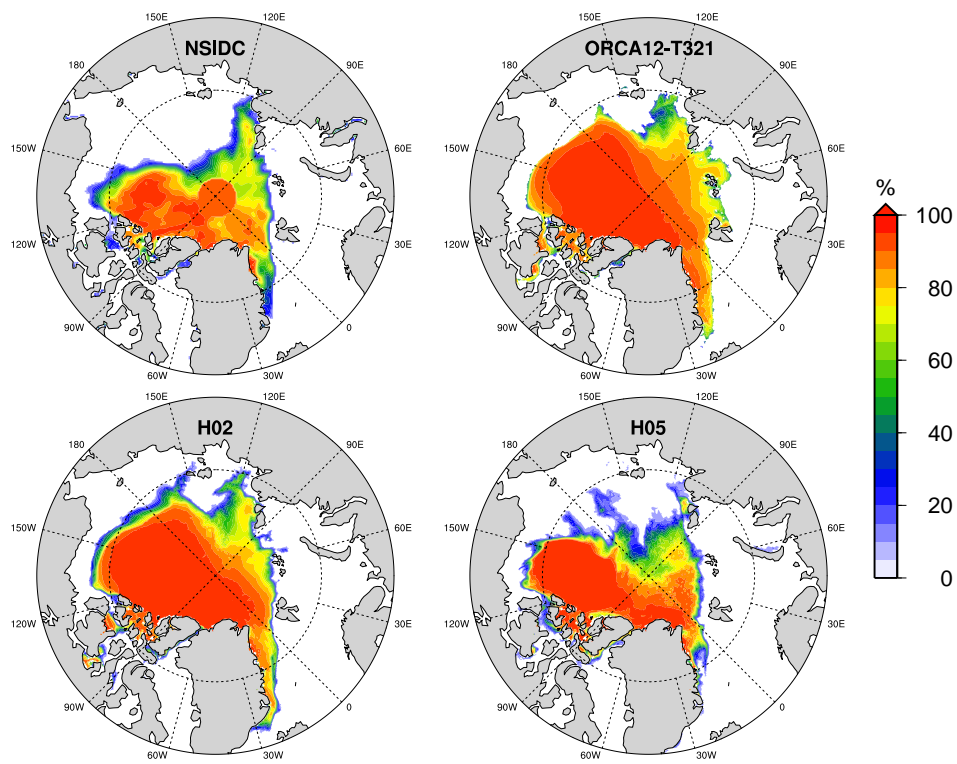


Figure 13. Ice concentration for September 2007 from NSIDC, the ORCA12 T321 run from Mercator Océan and CREG12 hindcasts H02 and H05.

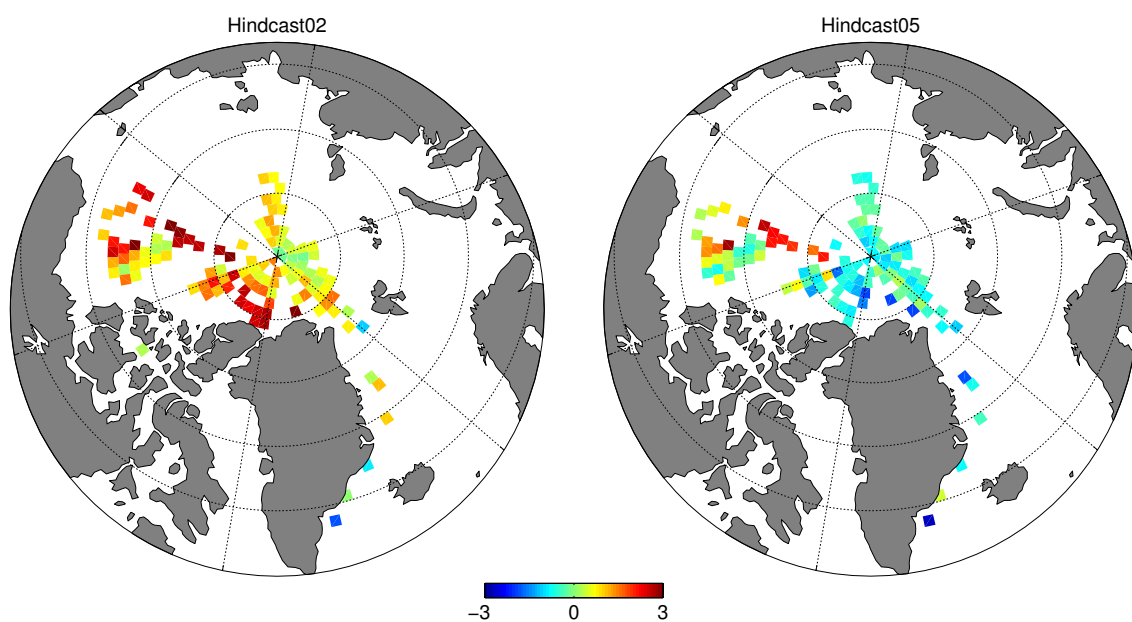


Figure 14. Difference (in m, model minus observation) between the sea ice thickness from hindcast H02 (left) and hindcast H05 (right) and measurements from ice mass balance buoys for the period 2003–2009 averaged across boxes measuring approximately 100km square.

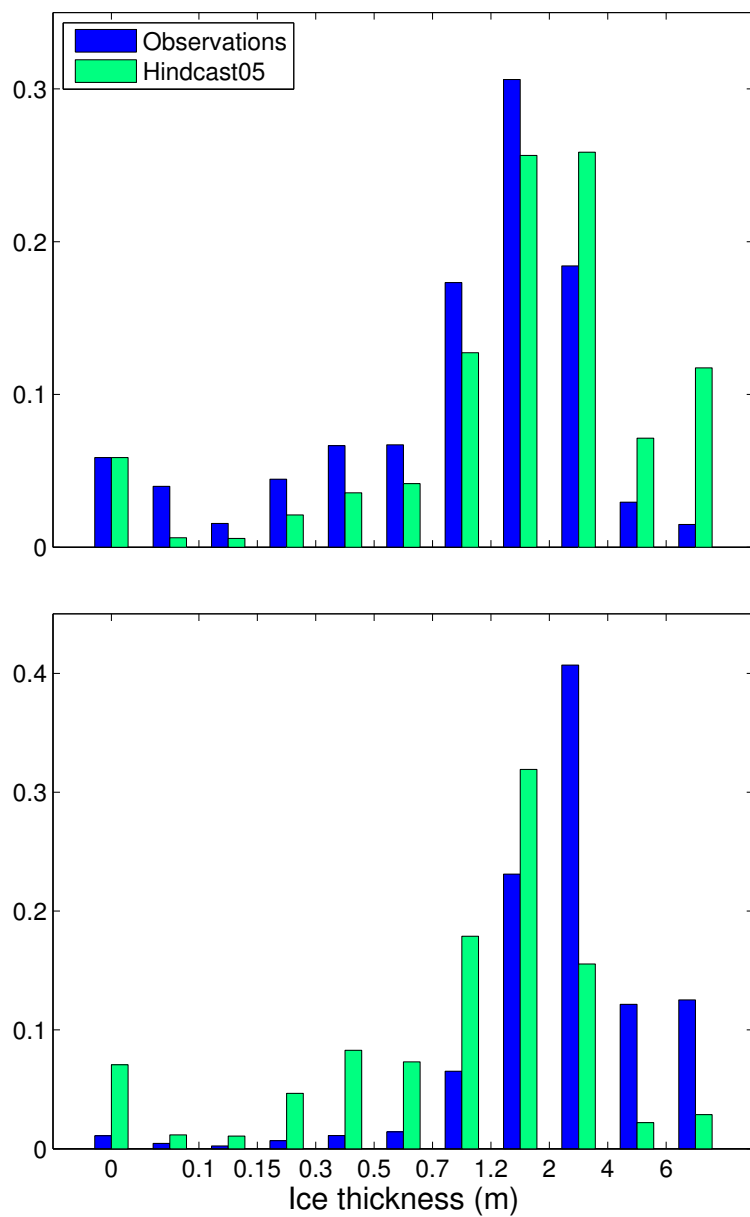


Figure 15. Average ice thickness distributions from ULS measurements (blue) and hindcast H05 (green) at the Beaufort Gyre Exploration Project mooring A (top) and at the North Pole Environmental Observatory mooring (bottom). The BGEP mooring data was averaged for the period September 2003 to December 2009. The NPEO mooring data was for the period Jan 2003 to Dec 2009 (but there are some gaps in the record). In each case the model output is averaged for the same period as the observations.

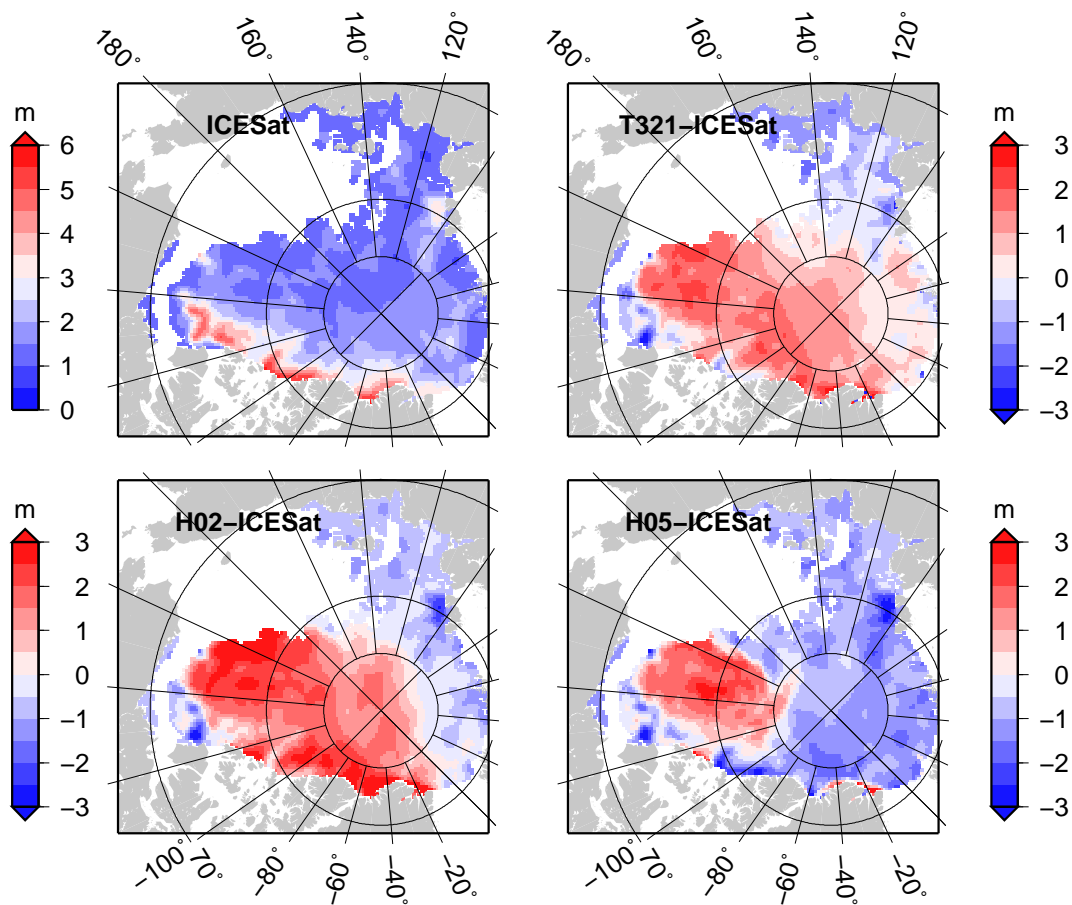


Figure 16. The mean ice thickness (in m) for October-November 2007 from ICESat, and the difference between ORCA12 T321 and CREG12 hindcasts H02 and H05 and the ICESat estimate.

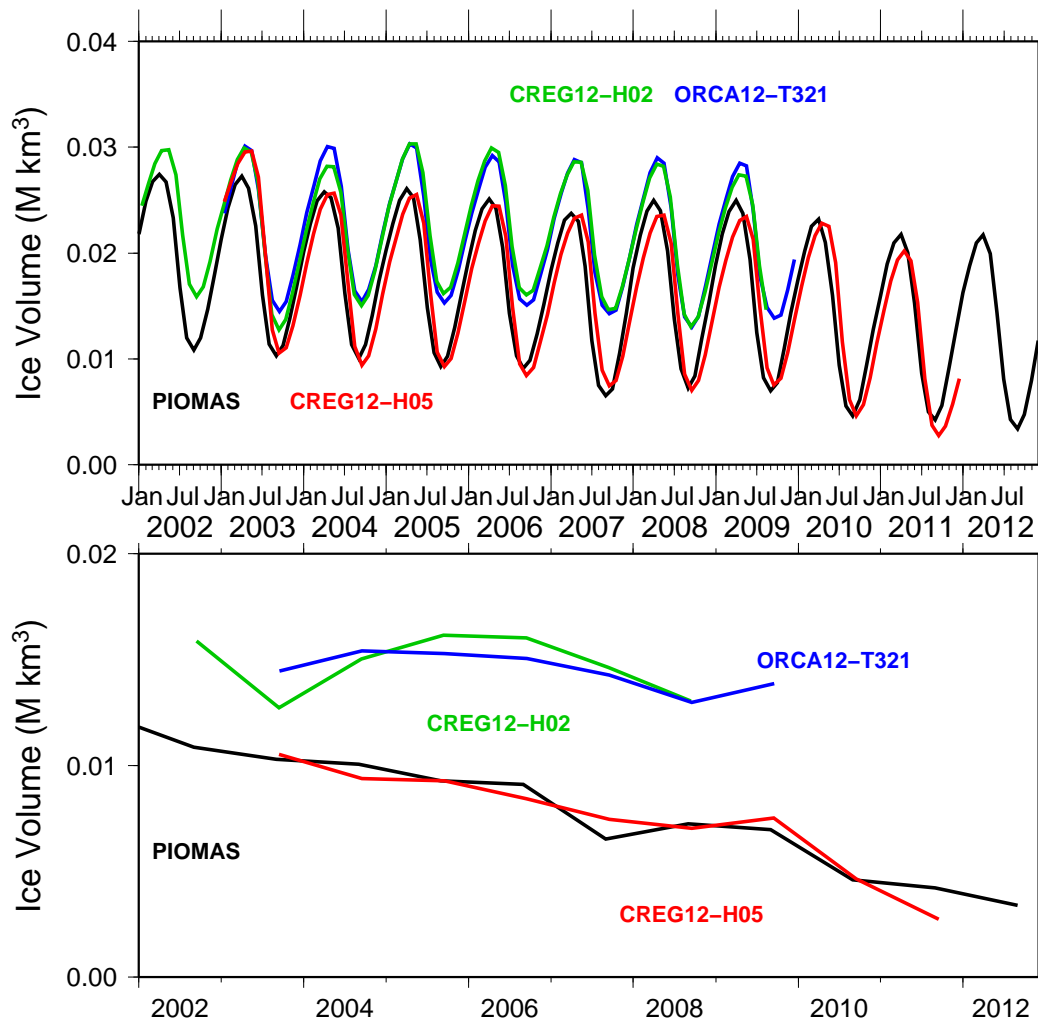


Figure 17. Monthly time series of total ice volume in the Arctic obtained from PIOMAS (black), the ORCA12 T321 run from Mercator Océan (blue), and CREG12 hindcasts H02 (green), and H05 (red). The top panel shows all months, the bottom panel retains only September from each year.

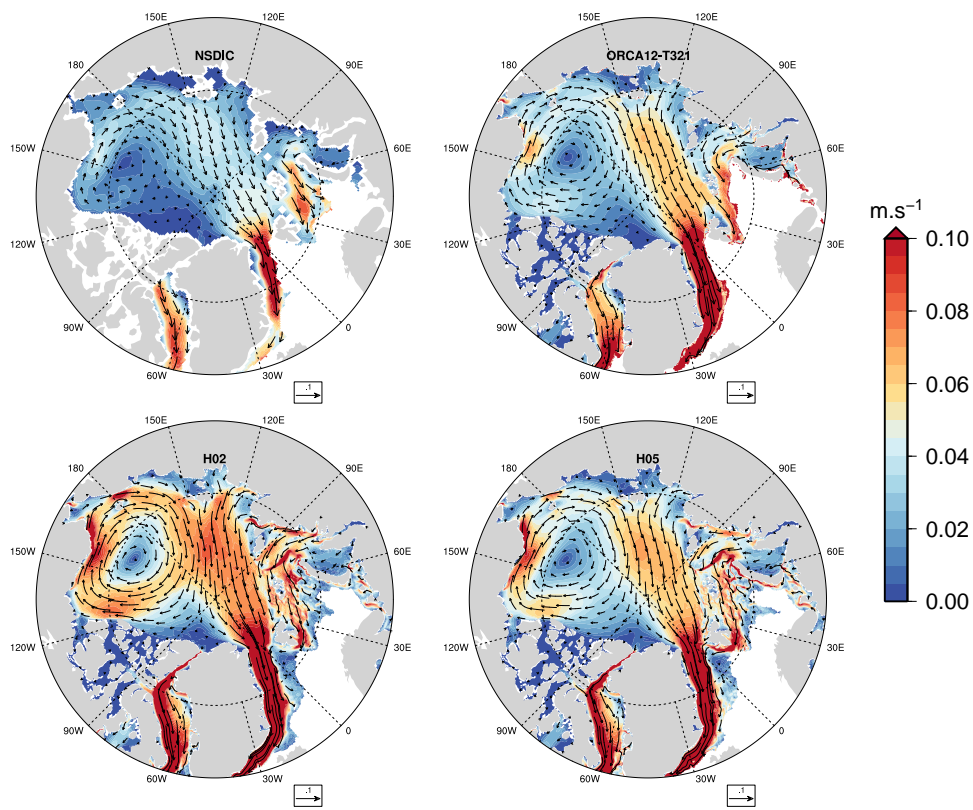


Figure 18. Average ice velocity (in m.s^{-1}) for March 2003-2008 from NSIDC, the ORCA12 T321 run from Mercator Océan, and CREG12 hindcasts H02 and H05.

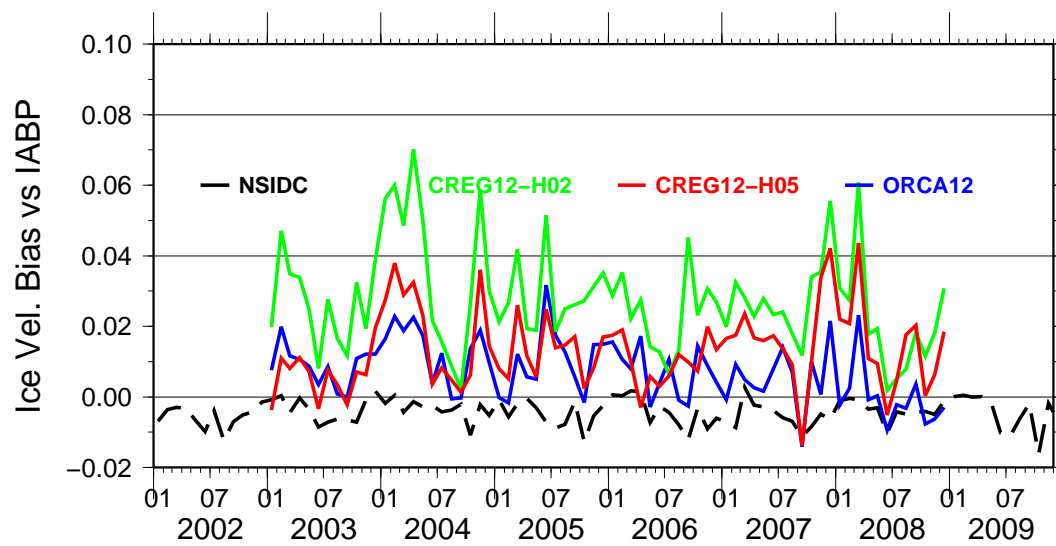


Figure 19. Monthly timeseries of average bias in monthly ice speed (in ms^{-1}) relative to IABP buoys for NSIDC (black dashed), the ORCA12 T321 run (blue), and CREG12 hindcasts H02 (green) and H05 (red).